J. Fluid Mech. (2010), *vol.* 644, *pp.* 165–192.
doi:10.1017/S0022112009992199

Universal solutions for Boussinesq and non-Boussinesq plumes

T. S. VAN DEN BREMER AND G. R. HUNT†

Department of Civil and Environmental Engineering, Imperial College London, Imperial College Road, London SW7 2AZ, UK

(Received 4 March 2009; revised 10 September 2009; accepted 11 September 2009)

Closed-form solutions describing the behaviour of buoyant axisymmetric turbulent rising plumes and fountains, emitted vertically from area sources in unconfined quiescent environments of uniform density, are proposed in a form that is universally applicable to Boussinesq and non-Boussinesq plumes. This paper, thereby, generalizes the results obtained separately for steady Boussinesq and non-Boussinesq plumes, including asymptotic virtual source corrections. The flux balance parameter $\Gamma = \Gamma(z)$, a local Richardson number, is instrumental in describing the behaviour of steady plumes and the initial rise behaviour of fountains with height z. Non-dimensional graphs (cf. the 'scale diagrams' of Morton & Middleton, *J. Fluid Mech.*, vol. 58, 1973, pp. 165–176) are plotted, showing certain characteristic heights for different source conditions, characterized by one single source flux balance parameter, giving a unique representation of the behaviour of Boussinesq fountains and both Boussinesq and non-Boussinesq plumes. Finally, a length scale has been identified that characterizes the height over which non-Boussinesq effects are important for lazy plumes rising from area sources.

1. Introduction

Plumes that have a sufficiently large density contrast with the fluid into which they are released are classified as non-Boussinesq. For these releases the Boussinesq approximation (see Turner 1979) is not valid. In the non-Boussinesq case the effects of variations in density on the flux of momentum and on the rate of entrainment are significant and must be taken into account. The behaviour of the plume or fountain with height is determined by the relative values of the source volume flux, source momentum flux and source buoyancy flux. The local momentum flux reduces with height in a rising fountain and increases with height for a plume – in each case as the buoyancy force does work. Entrainment of ambient fluid is responsible for an increase of volume flux and a decrease in density contrast with height for both plumes and fountains. Thence plumes that are non-Boussinesq at the source can be classified as Boussinesq at a certain height.

The conservation equations for Boussinesq plumes were formulated and solved for fully self-similar plumes rising from point sources by Morton, Taylor & Turner (1956). Central to the model of Morton *et al.* (1956) is the entrainment assumption, which

† Email address for correspondence: gary.hunt@imperial.ac.uk

states that the radial entrainment velocity at the edge of the plume u_e is proportional to the vertical velocity of the plume fluid w, i.e. $u_e = \alpha w$, where the constant of proportionality α, referred to as the entrainment coefficient, is independent of height. Morton (1959) went on to solve the conservation equations for plumes and fountains rising from area sources. The scale diagrams of Morton & Middleton (1973) that show certain characteristic scaled heights for different source conditions, as characterized by a single source flux balance parameter Γ_0, greatly assist in elucidating the results of Morton (1959). The source flux balance parameter as defined by Morton (1959) for the Boussinesq case is given by

$$\Gamma_0 = \frac{5B_0Q_0^2}{8\alpha\sqrt{\pi}M_{B,0}^{5/2}}, \tag{1.1}$$

where B_0 is the source buoyancy flux; Q_0 is the source volume flux; $M_{B,0}$ is the source momentum flux under the Boussinesq approximation (see §§ 2.1 and 2.2); and the subscript 0 denotes the source value. The source parameter Γ_0 can be used to distinguish three classes of solutions to the plume conservation equations: fountains ($\Gamma_0 < 0$) with source fluxes of buoyancy and momentum acting in opposing directions, forced plumes ($0 < \Gamma_0 < 1$) dominated by their source momentum flux for heights up to the order of a jet length and lazy plumes ($\Gamma_0 > 1$), which may be regarded as having a deficit of source momentum flux or, alternatively, an excess of mass flux (non-Boussinesq case) or volume flux (Boussinesq case) at the source compared with a pure plume. The characteristic heights plotted by Morton & Middleton (1973) include the initial rise height for fountains, a height characterizing the transition from jet-like to plume-like behaviour for forced plumes, heights corresponding to a maximum velocity and a minimum radius for lazy plumes and virtual and asymptotic virtual source corrections for both forced and lazy plumes. By applying the asymptotic virtual source correction as a vertical origin offset, the solutions for plumes rising from area sources developed by Morton (1959) can be replaced by the much simpler power-law solutions for plumes rising from point sources; the power-law solutions will match the original solution in the far field. The virtual source is merely the first step in a two-step procedure originally developed by Morton (1959) to locate the asymptotic virtual source (see § 5.1).

Hunt & Kaye (2001) provided a simplified method of finding the asymptotic virtual source correction for lazy Boussinesq plumes and validated against experimental measurements. Bloomfield & Kerr (2000) extended the original work on fountains by Morton (1959) and developed a theoretical model that quantifies both the entrainment of ambient fluid into the initial fountain upflow and the entrainment of fluid from the upflow and the environment in the subsequently formed annular downflow around the rising fountain core. To describe the relative importance of the fluxes of volume, momentum and buoyancy for a Boussinesq plume Hunt & Kaye (2005) expressed the parameter Γ, originally proposed by Morton (1959) as a source parameter, as a function of height z. The plume conservation equations were then written in terms of $\Gamma(z)$ and closed-form solutions to the conservation equations for Boussinesq plumes obtained focusing on lazy source conditions. For Boussinesq fountains Kaye & Hunt (2006) adopted a similar approach to find expressions for the initial rise height and thereby classified fountain behaviour into three regimes depending on the source parameter Γ_0.

Different approaches to solve for non-Boussinesq plumes have been proposed by Fannelop & Webber (2003) and Carlotti & Hunt (2005). Both considered plumes arising from area sources and solved for the fluxes of mass and momentum as a

function of scaled height. Both their approaches are an extension of the earlier and first systematic work on non-Boussinesq plumes by Rooney & Linden (1996), who derived solutions for the plume quantities as power-law functions of height on the basis of self-similarity considerations for slender non-Boussinesq plumes arising from point sources. Rooney & Linden (1996) used their self-similarity model to justify a modified entrainment assumption for non-Boussinesq plumes that has been confirmed experimentally by Ricou & Spalding (1961) amongst others and was first proposed by Morton (1965) based on the experimental results of Ricou & Spalding (1961). In this modified entrainment model the reduced entrainment that is observed for plumes with large density contrasts between the plume and ambient fluids is accommodated by an entrainment velocity u_e that is proportional to the product of the vertical plume velocity w and the square root of the local density contrast η, i.e. $u_e = \alpha w \sqrt{\eta}$. The density contrast $\eta = \rho/\rho_a$ is defined as the ratio of the plume density ρ and the ambient density ρ_a. Woods (1997) rewrote the solutions of Rooney & Linden (1996) and identified a characteristic length scale on which the transition to a Boussinesq plume takes place, beginning from a pure point source plume that is non-Boussinesq at the source. In addition, Woods (1997) discussed the difference in behaviour between Boussinesq and non-Boussinesq plumes. Carlotti & Hunt (2005) also evaluated asymptotic virtual source corrections for both lazy and forced non-Boussinesq plumes.

Although a significant share of the theoretical models that exist for plumes and fountains, including the works of all the aforementioned authors, has been developed for a constant entrainment coefficient α, there is convincing evidence that α is not a universal constant. Buoyancy-enhanced turbulence can explain why the value of the entrainment coefficient for plumes is significantly larger than the entrainment coefficient for jets (see for example Kaminski, Tait & Carazzo 2005 for a review). We return to a discussion of the entrainment coefficient in § 2.3.

More recently, a time-dependent implementation of the model of Morton *et al.* (1956) has been produced by Scase, Caulfield & Dalziel (2006*a*, 2008) and Scase *et al.* (2006*b*). The local implications of the conservation equations of Morton *et al.* (1956) have been investigated by Scase *et al.* (2007), who pointed out inconsistencies in the velocity field at the plume boundary and resolved these using a two-fluid model tracking both the evolution of the plume and the ambient fluids.

The current paper proposes a closed-form solution of the established plume conservation equations that can be used to describe both Boussinesq and non-Boussinesq rising plumes and Boussinesq fountains from area sources, and in so doing it aims to clarify the equivalence of the previously identified models describing Boussinesq and non-Boussinesq plumes. It thereby generalizes the results of a significant body of work including the contributions from Morton (1959), Morton & Middleton (1973), Hunt & Kaye (2001, 2005), Fannelop & Webber (2003), Carlotti & Hunt (2005) and Kaye & Hunt (2006) on both steady turbulent axisymmetric Boussinesq and non-Boussinesq plumes and the initial rise behaviour of Boussinesq fountains in unstratified quiescent environments. In congruence with the work of these authors a constant entrainment coefficient α has been adopted herein. The paper seeks to elucidate these results by plotting scale diagrams showing certain characteristic heights, including (asymptotic) virtual source corrections for different source conditions equivalent to the diagrams plotted by Morton & Middleton (1973) for Boussinesq plumes and fountains but herein in a form valid for both Boussinesq and non-Boussinesq plumes. By plotting contours corresponding to constant values of Γ and to constant values of the rate of change of Γ with height, as functions of the source parameter Γ_0, the behaviour of plumes and fountains is further clarified.

Furthermore, a characteristic height describing the transition from non-Boussinesq to Boussinesq behaviour as the plume ascends is proposed for lazy area sources, thereby extending the work of Woods (1997).

The paper is laid out as follows: § 2 introduces the plume conservation equations and rewrites these in a non-dimensional form that is universally applicable to Boussinesq and non-Boussinesq plumes and Boussinesq fountains. Solutions for pure jets ($\Gamma_0 = 0, \eta_0 = 1$) and pure plumes ($\Gamma_0 = 1$) arising from area sources are presented in § 3, and solutions for fountains ($\Gamma_0 < 0$) and forced ($0 < \Gamma_0 < 1$) and lazy ($\Gamma_0 > 1$) plumes are outlined and discussed in § 4. Different characteristic heights are considered in § 5, and the discussion is aided by the presentation of scale diagrams. The length scale on which non-Boussinesq effects are important is developed in § 6. Conclusions are drawn in § 7. Furthermore, the definitions of the (asymptotic) virtual sources by Morton (1959) and Carlotti & Hunt (2005) and the definition of the initial rise height by Morton (1959) are rewritten in the non-dimensional form adopted throughout this paper and provided as an appendix, for reference and to enable full appreciation of the equivalence of the different solutions.

2. Plume model

2.1. *Conservation equations*

The most commonly adopted profiles to describe the time-averaged horizontal variation of vertical velocity and density in an axisymmetric plume are Gaussian and top-hat profiles. Adopting top-hat profiles, the equations expressing conservation of mass (2.1) and momentum (2.2) prior to applying the Boussinesq approximation can be written as follows:

$$\frac{d(\eta w b^2)}{dz} = 2bu_e, \tag{2.1}$$

$$\frac{d(\eta w^2 b^2)}{dz} = g(1-\eta)b^2, \tag{2.2}$$

where w denotes the vertical velocity in the plume, b the radius of the plume, η the ratio of the plume density ρ and the (constant) density of the ambient ρ_a and u_e the horizontal entrainment velocity at the edge of the plume. The coordinate z is measured vertically upwards from the source at $z = 0$; velocity and mass and volume fluxes are positive in this direction. It has been assumed in deriving the equation for conservation of momentum flux (2.2) that the plume is tall and thin, so that the radial pressure gradient may be shown to be much smaller than the gradient of pressure with height. The third equation that is required for closure (we implicitly assume an entrainment model will be applied to achieve turbulence closure) is that of conservation of volume flux. In the Boussinesq case, conservation of volume flux is implied by conservation of mass flux (2.1), since under the Boussinesq approximation the density terms on both sides of the equation may be ignored. Rooney & Linden (1996) employed thermodynamic arguments for an ideal gas to show that volume flux is also conserved in the non-Boussinesq case. In both cases conservation of volume takes the form

$$\frac{\mathrm{d}(wb^2)}{\mathrm{d}z} = 2bu_e. \tag{2.3}$$

The conservation equations (2.1)–(2.3) are also valid for fountains (see Bloomfield & Kerr 2000) and govern the behaviour until the initial maximum rise height is reached but not the subsequent collapse, as the dynamics of entrainment are then significantly

modified, and momentum is exchanged between upflowing and downflowing bodies of fluid. Combining conservation of volume flux (2.3) and conservation of mass flux (2.1) yields the conservation of the flux of density deficit, i.e. conservation of the quantity

$$B = \pi g(1-\eta)wb^2, \tag{2.4}$$

which has the dimensions of buoyancy flux L^4T^{-3} and becomes equal to the buoyancy flux in the Boussinesq limit. This quantity is conserved for both the Boussinesq and the non-Boussinesq cases.

As explained, the Boussinesq approximation provides a simplified but not strictly necessary route to conservation of volume. Under the Boussinesq approximation it is assumed that the effect of variations in density ratio η in the left-hand term of the momentum flux conservation equation (2.2) can be neglected; thence conservation of momentum flux under the Boussinesq approximation can be expressed as:

$$\frac{d(w^2b^2)}{dz} = g(1-\eta)b^2. \tag{2.5}$$

2.2. *The flux balance parameter* Γ

For top-hat profiles the fluxes of mass G, volume Q and momentum M are defined as

$$G = \pi\eta wb^2, \qquad Q = \pi wb^2, \qquad M = \pi\eta w^2b^2. \tag{2.6}$$

In the Boussinesq case the momentum flux is approximated by M_B:

$$M_B = \pi w^2b^2. \tag{2.7}$$

The flux balance parameter Γ is defined in (2.8) for the Boussinesq case (see Morton 1959; Hunt & Kaye 2001) and the non-Boussinesq case (see Carlotti & Hunt 2005):

$$\Gamma = \begin{cases} \dfrac{5BQ^2}{8\alpha\sqrt{\pi}M_B^{5/2}}, & \text{Boussinesq,} \\ \dfrac{5BG^2}{8\alpha\sqrt{\pi}M^{5/2}}, & \text{non-Boussinesq,} \end{cases} \tag{2.8}$$

where a constant entrainment coefficient α has been assumed by these authors. The flux balance parameter can be expressed as the square of the ratio of two length scales, namely the jet length L_J and the source length L_S, so that

$$\Gamma = \left(\frac{L_S}{L_J}\right)^2. \tag{2.9}$$

For the Boussinesq case and the non-Boussinesq case respectively these length scales are defined as (see Carlotti & Hunt 2005)

$$L_J = \begin{cases} \dfrac{\sqrt{10}}{3\pi^{1/4}\alpha^{1/2}}\dfrac{M_B^{3/4}}{B^{1/2}}, & \text{Boussinesq,} \\ \dfrac{\sqrt{10}}{3\pi^{1/4}\alpha^{1/2}}\dfrac{M^{3/4}}{B^{1/2}}, & \text{non-Boussinesq,} \end{cases} \qquad L_S = \begin{cases} \dfrac{5}{6\alpha\sqrt{\pi}}\dfrac{Q}{M_B^{1/2}}, & \text{Boussinesq,} \\ \dfrac{5}{6\alpha\sqrt{\pi}}\dfrac{G}{M^{1/2}}, & \text{non-Boussinesq.} \end{cases} \tag{2.10}$$

2.3. *Entrainment assumption*

The entrainment model adopted herein for Boussinesq plumes and fountains is the classical entrainment model originally proposed by Morton *et al.* (1956), which states

that the radial entrainment velocity u_e is proportional to the vertical velocity w. Despite its uncertain physical basis, the entrainment model of Morton *et al.* (1956) with an entrainment coefficient α that is independent of height has been adopted in a significant majority of the work on plumes and fountains (see for example Caulfield & Woods 1998, who considered plumes in non-uniformly stratified environments; Conroy & Llewellyn Smith 2008, who considered the effect of chemical reactions on plume behaviour; and Scase *et al.* 2006*a*, *b*, 2008, who generalized the model of Morton *et al.* 1956 to allow for time dependence in the various fluxes for both Boussinesq and non-Boussinesq plumes). Turner (1986) discussed further the development of the classical entrainment assumption and its applications to geophysical flows.

Based on the experimental results of Ricou & Spalding (1961), Morton (1965) showed that for plumes with a large source density contrast, the entrainment model must be modified by including a density contrast term:

$$u_e = \begin{cases} \alpha|w| & \text{for Boussinesq plumes and fountains,} \\ \alpha|w|\sqrt{\eta} & \text{for non-Boussinesq plumes,} \end{cases} \tag{2.11}$$

where the $|w|$ term ensures that the entrainment is always positive, which is required to model reversing plumes. Whilst it is clear that the basic conservation equations and the entrainment model cannot adequately describe the behaviour of a reversing plume, the $|w|$ term is retained to accommodate the (unphysical) definition of the virtual source for lazy plumes of Morton (1959) (see § 5.1). Furthermore, Morton *et al.* (1956) and Rooney & Linden (1996) showed that the entrainment models in (2.11) are consistent with similarity theory for Boussinesq and non-Boussinesq plumes, respectively.

In the modified entrainment assumption for non-Boussinesq plumes the additional $\sqrt{\eta}$ term accounts for the near-field reduction in spreading rate because of the reduction in the rate of entrainment that is observed in non-Boussinesq plumes (Morton 1965). By arguing that the entrainment process depends on the local Reynolds stress ($\propto \rho w^2$), Morton (1965) provided justification for the expression for the entrainment velocity u_e in (2.11). Although the number of experimental studies on entrainment in non-Boussinesq plumes is limited (Ricou & Spalding 1961; Thring & Newby 1953), the modified entrainment model has been applied extensively and predominantly to the ventilation of fires, which are characterized by a large source density contrast (see Rooney 1997; Linden 1999; Heskestad 1998). In an experimental study, Cetegen, Zukoski & Kubota (1984) showed that the modified entrainment assumption can be successfully applied to predict the mass fluxes in a fire plume. Woods (1997) investigated the theoretical implications of the modified entrainment assumption for downward-propagating non-Boussinesq plumes ($\eta > 1$), for which the modified entrainment assumption predicts enhanced instead of reduced entrainment. However, we note that the modified entrainment model is unlikely to be valid for non-Boussinesq fountains and downward-propagating plumes, as the physical grounds on which to expect enhanced entrainment owing to large density differences are not evident. The authors are not aware of modified entrainment models that have been proposed for non-Boussinesq fountains.

Although experimental measurements of the entrainment coefficient α vary considerably, there is extensive evidence to suggest that α is not a universal constant; namely the entrainment coefficient is significantly larger for plumes (α_p) than for jets (α_j), a phenomenon that can be explained by buoyancy-enhanced turbulence. Kaminski *et al.* (2005) showed that although different estimates for the entrainment

coefficients in jets are in close agreement and converge to an average value of $\alpha_j = 0.075$, it remains difficult to cite a definitive value for the entrainment coefficient in plumes. The values of the entrainment coefficient for plumes vary between $\alpha_p = 0.10$ in Baines (1983) and $\alpha_p = 0.16$ in Shabbir & George (1994), and this 60 % variation will inevitably have a non-negligible effect on the ability to predict fluxes at a given height (Kaminski *et al.* 2005). The values of the entrainment coefficients cited here are for top-hat velocity profiles consistent with the profiles assumed herein.

Based on experimental results, List & Imberger (1973) have shown that the spreading angle of forced plumes is virtually independent of height, which led these authors to conclude that the entrainment coefficient for forced plumes varies linearly with the local Richardson number. List & Imberger (1973) thereby confirmed the earlier result of Priestley & Ball (1955), who did not make an explicit entrainment assumption but instead assumed a particular form of the Reynolds stress distribution. More recently, Wang & Law (2002) have provided experimental verification of the linear variation of the entrainment coefficient with the local Richardson number for forced plumes. Kaminski *et al.* (2005) have proposed a similar linear parameterization but have introduced a third term that takes into account a self-similarity drift and aids the reconciliation of the different estimates of the entrainment coefficient found in the literature, as discussed further in Carazzo, Kaminski & Tait (2006). For fountains there is evidence that the entrainment coefficient is significantly reduced by negative buoyancy (Kaminski *et al.* 2005; Papanicolaou, Papakonstantis & Christodoulou 2008). Kaminski *et al.* (2005) showed that to first order this effect is well described by a linear dependence on the local (negative) Richardson number.

The validity of the entrainment model of Morton *et al.* (1956) is challenged on a more fundamental level in regions of strong flow development, for which the vertical length scale on which changes in the flow behaviour take place is not significantly larger than the radius of the release at that height (cf. Kaye 2008). For regions characterized by a rapid change of the flow behaviour with height the radial pressure is no longer much smaller than the vertical pressure gradient, violating an assumption made in deriving the plume equations of Morton *et al.* (1956). Examples of regions for which the entrainment model of Morton *et al.* (1956) is invalid are found at the top of fountains, where the vertical velocity drops to zero, but the turbulent field and hence entrainment persists (cf. Cardoso & Woods 1993), and in the near-source region of very lazy plumes ($\Gamma_0 \gg 1$), where the slope of the plume envelope becomes very large as the plume contracts. The former applies especially to very weak fountains ($\Gamma_0 \ll -1$), for which the (initial) rise height is of the same order of magnitude or smaller than the source radius.

Despite convincing evidence that the entrainment coefficient is not a universal constant and that, particularly for forced plumes, an improved fit to the experimental data can be obtained for an entrainment coefficient that varies linearly with the local flux balance parameter Γ, a constant entrainment coefficient has been assumed herein. It is the aim of this paper to generalize a large body of work with contributions from various authors, who have invariably adopted an entrainment model with a constant entrainment coefficient.

2.4. *General form of plume equations*

To facilitate the formulation of one unique set of equations valid for both Boussinesq and non-Boussinesq plumes, a new parameter, namely the effective entrainment radius β, is now introduced. The effective entrainment radius is equal to the radius b for the Boussinesq case and equal to the product of the radius and the square root of the

density contrast, i.e. $b\sqrt{\eta}$, in the non-Boussinesq case. Adopting this new parameter, the flux balance parameter $\Gamma = \Gamma(z)$ takes the form

$$\Gamma(z) = \frac{5g(1-\eta(z))\beta(z)}{8\alpha w(z)|w(z)|\eta(z)}, \tag{2.12}$$

where the $|w(z)|$ term is introduced to aid the definition of the virtual source of lazy plumes (see § 5.1). After considerable manipulation the three conservation equations (2.1)–(2.3) can be represented in terms of the non-dimensional parameter Γ, the non-dimensional effective entrainment radius $\hat{\beta} = \beta/\beta_0$, the non-dimensional vertical velocity $\hat{w} = w/w_0$ and a non-dimensional height $\zeta = 4\alpha z/\beta_0$:

$$\frac{\mathrm{d}\Gamma}{d\zeta} = \frac{\Gamma(1-\Gamma)}{\hat{\beta}}\mathrm{sign}(w), \tag{2.13}$$

$$\frac{\mathrm{d}\hat{\beta}}{\mathrm{d}\zeta} = \frac{1}{5}\left(\frac{5}{2} - \Gamma\right)\mathrm{sign}(w), \tag{2.14}$$

$$\frac{\mathrm{d}\hat{w}}{\mathrm{d}\zeta} = \frac{2}{5}\frac{\hat{w}}{\hat{\beta}}\left(\Gamma - \frac{5}{4}\right)\mathrm{sign}(w). \tag{2.15}$$

Although the plume quantities can be scaled on their respective values at any one height, scaling on their respective source values, denoted by the subscript 0, is adopted herein. One advantage of this formulation of the conservation equations is that the bulk plume and fountain behaviour at any height is captured through the parameter Γ. Solving for $\Gamma(\zeta)$ immediately reveals the plume or fountain behaviour with height.

A closed-form solution to the system of ordinary differential equations (2.13)–(2.15) can be found subject to the source conditions $\Gamma = \Gamma_0$, $\hat{\beta} = 1$ and $\hat{w} = 1$ at $\zeta = \zeta_0 = 0$. There are five distinct classes of solution for plumes arising from finite area sources, depending on the source value of the parameter Γ: fountains ($\Gamma_0 < 0$), pure jets ($\Gamma_0 = 0$), forced plumes ($0 < \Gamma_0 < 1$), pure plumes ($\Gamma_0 = 1$) and lazy plumes ($\Gamma_0 > 1$). Within the fountain solution class, Kaye & Hunt (2006) provided a sub-classification of highly forced ($-1 \ll \Gamma_0 < 0$) and weak fountains ($\Gamma_0 \ll -1$), for which different limiting cases of the solution for the initial rise height apply (see also Lin & Armfield 2000). Regarding the subdivision into the forced, pure and lazy regimes, it should be noted that a plume with given fluxes can be classed under a different solution regime, depending on whether it is described by a Boussinesq or a non-Boussinesq model. Hunt & Kaye (2005) introduced an off-source buoyancy flux gain and showed that of these different classes of solution only two are steady, namely the stable pure plume and the unstable pure jet solution, which will become unsteady in the case of even small deviations away from $\Gamma = 0$ at, or above, the source.

Self-similar plumes from point sources constitute one further class of solution to the conservation equations. Such solutions have been derived by Morton *et al.* (1956) for Boussinesq plumes and by Rooney & Linden (1996) for non-Boussinesq plumes. For reference and to facilitate comparison with the solutions for plumes rising from area sources their solutions, rewritten for consistency using the notation adopted herein, are given in Appendix A.

To describe the behaviour of the density contrast η it is convenient to introduce

$$\Delta = \begin{cases} 1-\eta, & \text{Boussinesq,} \\ \dfrac{1-\eta}{\eta}, & \text{non-Boussinesq.} \end{cases} \tag{2.16}$$

The corresponding definition of Γ is

$$\Gamma = \frac{5g}{8\alpha}\frac{\beta\Delta}{w|w|}, \tag{2.17}$$

where β, Δ and w are all functions of height ζ. Solutions of the non-dimensional conservation equations (2.13)–(2.15) can be found in terms of the effective entrainment radius β, the vertical velocity w and the density parameter Δ.

3. Pure plumes ($\Gamma_0 = 1$) and pure jets ($\Gamma_0 = 0$, $\eta_0 = 1$)

3.1. *Pure jets from area sources*

For releases arising from finite non-zero area sources, $\Gamma_0 = 0$ must correspond to $\eta_0 = \eta(z) = 1$, i.e. a pure jet with zero buoyancy flux. For a pure jet, (2.13) requires that $\Gamma = \Gamma_0 = 0$ for all heights. Equations (2.14) and (2.15) give the recognizable solutions for b and w:

$$\frac{b}{b_0} = 1 + \frac{2\alpha}{b_0}z, \qquad \frac{w}{w_0} = \frac{1}{1 + \frac{2\alpha}{b_0}z}. \tag{3.1}$$

3.2. *Pure plumes from area sources*

For pure plumes arising from finite non-zero area sources, (2.13) requires that $\Gamma = \Gamma_0 = 1$ for all heights. Equations (2.14) and (2.15) combined with the definition of Γ (2.17) give the respective solutions for β, w and Δ:

$$\frac{\beta}{\beta_0} = \frac{3}{10}\left(\frac{10}{3} + \zeta\right), \quad \frac{w}{w_0} = \left(\frac{10}{3}\right)^{1/3}\left(\frac{10}{3} + \zeta\right)^{-1/3}, \quad \frac{\Delta}{\Delta_0} = \left(\frac{10}{3}\right)^{5/3}\left(\frac{10}{3} + \zeta\right)^{-5/3}. \tag{3.2}$$

These solutions are equivalent to those for pure plumes from point sources (see Appendix A) with an origin correction of $\zeta_{avs} = -10/3$.

4. Fountains ($\Gamma_0 < 0$), forced plumes ($0 < \Gamma_0 < 1$) and lazy plumes ($\Gamma_0 > 1$)

Equations (2.13) and (2.14) can be solved simultaneously to give the effective entrainment radius β for different properties of flow at the source as characterized by Γ_0 for fountains ($\Gamma_0 < 0$), forced plumes ($0 < \Gamma_0 < 1$) and lazy plumes ($\Gamma_0 > 1$):

$$\frac{\beta}{\beta_0} = \sqrt{\frac{\Gamma}{\Gamma_0}}\left(\frac{1-\Gamma_0}{1-\Gamma}\right)^{3/10}. \tag{4.1}$$

Substituting (4.1) back into (2.13) gives the rate of change of the flux balance parameter with height:

$$\frac{\mathrm{d}\Gamma}{\mathrm{d}\zeta} = \Gamma(1-\Gamma)\sqrt{\frac{\Gamma_0}{\Gamma}}\left(\frac{1-\Gamma}{1-\Gamma_0}\right)^{3/10}\mathrm{sign}(w). \tag{4.2}$$

Integrating (4.2) gives the height ζ at which a given value of Γ is attained:

$$\zeta = \begin{cases} -\frac{(1-\Gamma_0)^{3/10}}{\sqrt{-\Gamma_0}} \displaystyle\int_{\Gamma_0}^{\Gamma} \frac{d\Gamma}{\sqrt{-\Gamma}(1-\Gamma)^{13/10}} & \text{for } \Gamma < 0, \\ \frac{(1-\Gamma_0)^{3/10}}{\sqrt{\Gamma_0}} \displaystyle\int_{\Gamma_0}^{\Gamma} \frac{d\Gamma}{\sqrt{\Gamma}(1-\Gamma)^{13/10}} & \text{for } 0 < \Gamma < 1, \\ -\frac{(\Gamma_0-1)^{3/10}}{\sqrt{\Gamma_0}} \displaystyle\int_{\Gamma_0}^{\Gamma} \frac{d\Gamma}{\sqrt{\Gamma}(\Gamma-1)^{13/10}} & \text{for } \Gamma > 1. \end{cases} \tag{4.3}$$

Finally, combining the second and the third conservation equation ((2.14) and (2.15)) yields the vertical velocity:

$$\frac{w}{w_0} = \sqrt{\frac{\Gamma_0}{\Gamma}} \left(\frac{1-\Gamma}{1-\Gamma_0} \right)^{1/10}. \tag{4.4}$$

Combining the solutions for β (4.1) and w (4.4) and the definition of Γ (2.17), Δ can be expressed as

$$\frac{\Delta}{\Delta_0} = \sqrt{\frac{\Gamma_0}{\Gamma}} \sqrt{\frac{1-\Gamma}{1-\Gamma_0}}. \tag{4.5}$$

The solutions for β (4.1), w (4.4) and Δ (4.5) can be combined to give solutions for the fluxes of mass, volume and momentum for the Boussinesq and non-Boussinesq cases separately (see Appendix B). For convenience we introduce $\mathscr{G} = \pi w \beta^2$ and $\mathscr{M} = \pi w^2 \beta^2$, where $\mathscr{G}$ denotes the mass flux (G) in the non-Boussinesq case and the volume flux (Q) in the Boussinesq case and $\mathscr{M}$ the momentum flux (M) in the non-Boussinesq case and the approximate momentum flux (M_B) in the Boussinesq case. By combining (4.1) and (4.4) the non-dimensional fluxes $\hat{\mathscr{G}}$ and $\hat{\mathscr{M}}$ can be expressed as

$$\hat{\mathscr{G}} = \frac{\mathscr{G}}{\mathscr{G}_0} = \sqrt{\frac{\Gamma}{\Gamma_0}} \sqrt{\frac{1-\Gamma_0}{1-\Gamma}}, \qquad \hat{\mathscr{M}} = \frac{\mathscr{M}}{\mathscr{M}_0} = \left(\frac{1-\Gamma_0}{1-\Gamma} \right)^{2/5}. \tag{4.6}$$

The rates of change of $\hat{\mathscr{G}}$ and $\hat{\mathscr{M}}$ with height can be found by combining their derivatives with respect to Γ with $\mathrm{d}\Gamma/\mathrm{d}\zeta$ from (4.2):

$$\frac{\mathrm{d}\hat{\mathscr{G}}}{\mathrm{d}\zeta} = \frac{1}{2} \left(\frac{1-\Gamma_0}{1-\Gamma} \right)^{1/5}, \quad \frac{\mathrm{d}\hat{\mathscr{M}}}{\mathrm{d}\zeta} = \mathrm{sign}(\Gamma) \frac{2}{5} \sqrt{\Gamma_0 \Gamma} \left(\frac{1-\Gamma_0}{1-\Gamma} \right)^{1/10}. \tag{4.7}$$

It is clear from (4.2) that for forced plumes Γ increases monotonically with height from its source value Γ_0 and asymptotically converges to $\Gamma = 1$ from below, whereas for lazy plumes Γ decreases monotonically from Γ_0, asymptotically converging to $\Gamma = 1$ from above. For fountains, Γ decreases from its (negative) source value with increasing height. The limit $\Gamma \to -\infty$ corresponds to the initial rise height ζ_{irh} of the fountain, and at that height the fountain will reverse direction. Figures 1 and 2 illustrate the behaviour of Γ with height by showing contours of constant Γ and $\mathrm{d}\Gamma/\mathrm{d}\zeta$ in (Γ_0, ζ) space. For a given Γ_0 in figures 1(a) and 2(a) the vertical distance between the $\zeta = 0$ axis and a given contour of constant Γ indicates the vertical distance within the plume or fountain required for the flux balance parameter to decrease (or increase) from the chosen source value to that constant. It is evident then from figure 2 that for lazy plumes the lazier the plume is at its source (i.e. for increasingly large Γ_0), the larger the rate of convergence to the pure plume limit $\Gamma = 1$ and that for sufficiently lazy plumes ($\Gamma_0 \gtrsim 10$) the lazier the plume, the smaller the height over which a given value of Γ is attained. It is clear from figure 1 that

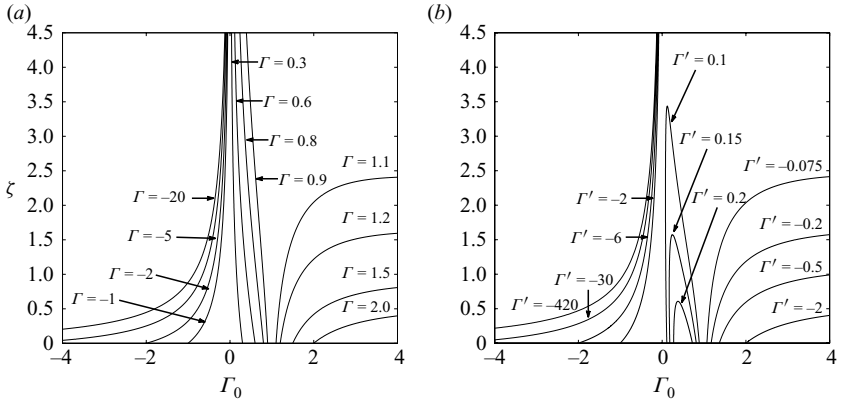

FIGURE 1. Contours of (a) constant Γ and (b) constant $\mathrm{d}\Gamma/\mathrm{d}\zeta$, denoted by Γ', for fountains, forced and lazy plumes.

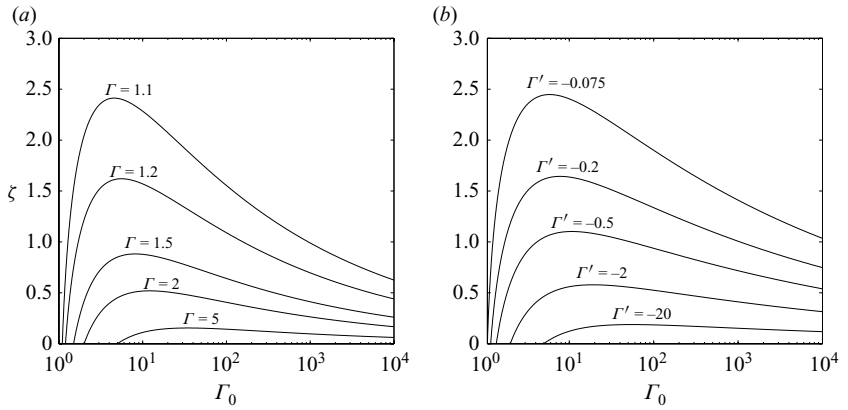

FIGURE 2. Contours of (a) constant Γ and (b) constant $\mathrm{d}\Gamma/\mathrm{d}\zeta$, denoted by Γ', for (very) lazy plumes.

in general, the height over which Γ converges to $\Gamma = 1$ is much larger for forced plumes than for lazy plumes. For fountains, figure 1 shows that the rate at which $\Gamma \to -\infty$ increases in accordance with the laziness of the fountain at its source (i.e. for increasingly negative Γ_0).

To enable interpretation of figures 1 and 2 it is instructive to consider lazy plumes as having a deficit of source momentum flux or, alternatively, an excess of mass flux (non-Boussinesq case) or volume flux (Boussinesq case) at the source compared with a pure plume. For forced plumes the reverse is true. A third way in which large (positive) values of Γ_0 can be obtained is by increasing the density contrast at the source η_0. As the vertical scaling is a function of η_0 in the non-Boussinesq case, care needs to be taken when interpreting figures 1 and 2 for comparison between plumes and fountains with different values for the source density contrast η_0.

Owing to entrainment of ambient fluid the density contrast η for plumes will increase monotonically from its source value η_0, asymptotically converging to $\eta = 1$ with height, whereas for fountains η will decrease monotonically with height but will reach a value $1 \leqslant \eta < \eta_0$ at the initial rise height, depending on the source conditions Γ_0 and η_0. Expressed in terms of the density parameter $\hat{\Delta} = \Delta/\Delta_0$, it is evident that $\hat{\Delta}$ will decrease monotonically from its source value $\hat{\Delta} = 1$ and converge to its

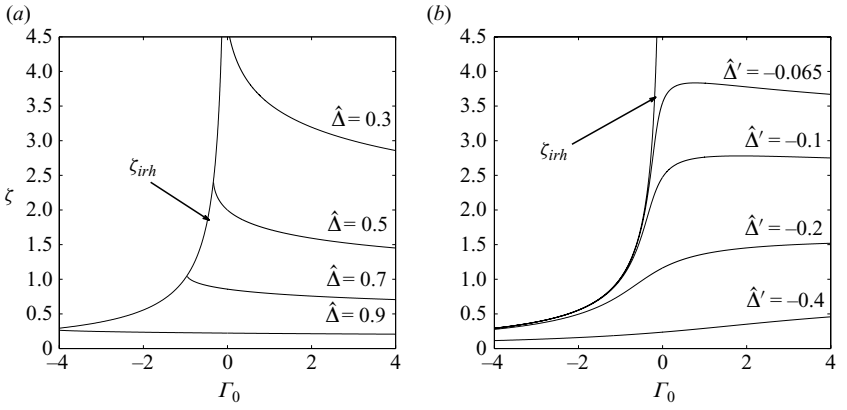

FIGURE 3. Contours of (a) constant $\hat{\Delta}$ and (b) constant $\mathrm{d}\hat{\Delta}/\mathrm{d}\zeta$, denoted by $\hat{\Delta}'$, for fountains, forced and lazy plumes.

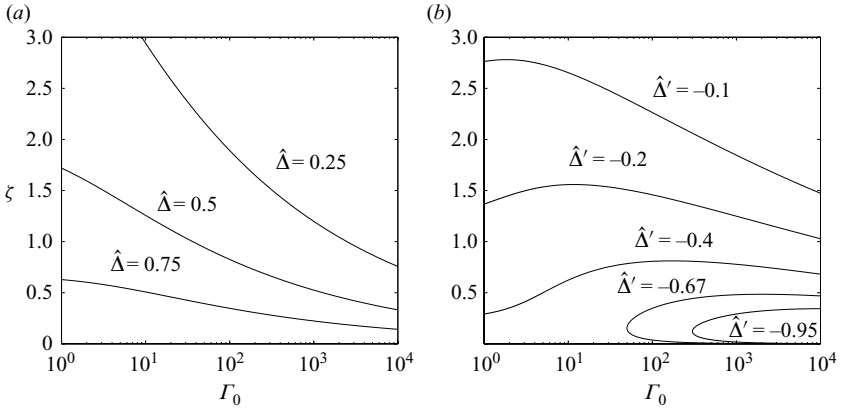

FIGURE 4. Contours of (a) constant $\hat{\Delta}$ and (b) constant $\mathrm{d}\hat{\Delta}/\mathrm{d}\zeta$, denoted by $\hat{\Delta}'$, for (very) lazy plumes.

asymptotic value $\hat{\Delta}=0$ with height for plumes, whereas for fountains $\hat{\Delta}$ will also decrease monotonically with height from its source value $\hat{\Delta}=1$ but will, according to (4.5), reach a value of $\hat{\Delta}=\sqrt{\Gamma_0/(\Gamma_0-1)}$ at the initial rise height ($\Gamma=-\infty$). The rate of change of $\hat{\Delta}$ with height can be found by combining the derivative of (4.5) with respect to Γ and $\mathrm{d}\Gamma/\mathrm{d}\zeta$ from (4.2):

$$\frac{\mathrm{d}\hat{\Delta}}{\mathrm{d}\zeta}=-\frac{1}{2}\frac{\Gamma}{\Gamma_0}\left(\frac{1-\Gamma}{1-\Gamma_0}\right)^{4/5}. \tag{4.8}$$

Figures 3 and 4 illustrate the behaviour of $\hat{\Delta}$ with height by showing contours of constant $\hat{\Delta}$ and $\mathrm{d}\hat{\Delta}/\mathrm{d}\zeta$ in the (Γ_0,ζ) space. From (4.5) and (4.8), respectively, the horizontal axes in figures 3 and 4 correspond to $\hat{\Delta}|_{\zeta=0}=1$ in panel (a) of both the figures and to $\mathrm{d}\hat{\Delta}/\mathrm{d}\zeta|_{\zeta=0}=-1/2$ in panels (b) of both the figures. It is evident then from figure 3 that the behaviour of $\hat{\Delta}$ is relatively independent of Γ_0 for forced and moderately lazy plumes. Moreover, it is evident from figure 3 that only for forced fountains is the density contrast significantly diluted relative to the source contrast before the fountain reaches its initial rise height (a height marked as ζ_{irh}). For lazy plumes, figure 4 shows that the density contrast is dissipated over a much smaller

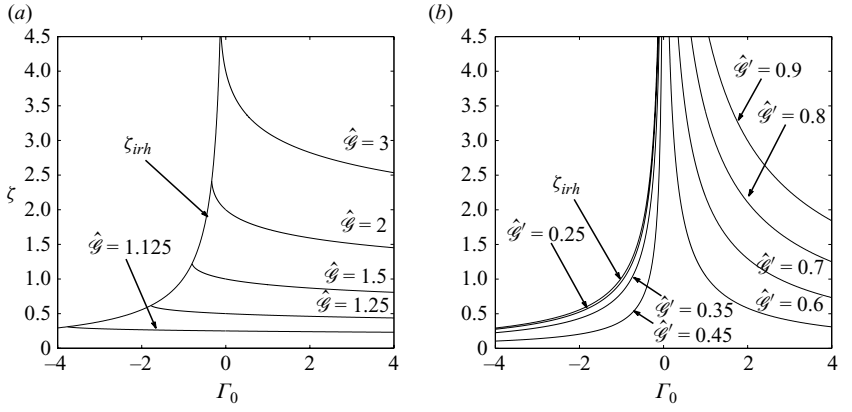

FIGURE 5. Contours of (*a*) constant $\hat{\mathcal{G}}$ and (*b*) constant $\mathrm{d}\hat{\mathcal{G}}/\mathrm{d}\zeta$, denoted by $\hat{\mathcal{G}}'$, for fountains, forced and lazy plumes.

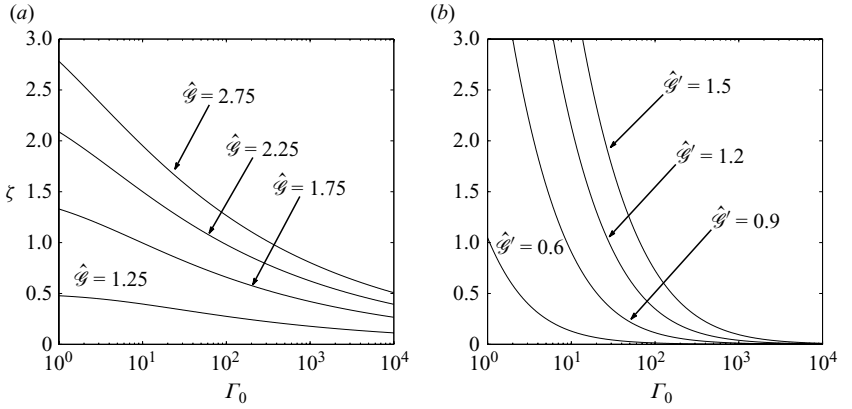

FIGURE 6. Contours of (*a*) constant $\hat{\mathcal{G}}$ and (*b*) constant $\mathrm{d}\hat{\mathcal{G}}/\mathrm{d}\zeta$, denoted by $\hat{\mathcal{G}}'$, for (very) lazy plumes.

height in accordance with the laziness of the plume (i.e. for increasingly large Γ_0). It can be shown by differentiating (4.8) with respect to Γ that for sufficiently lazy plumes ($\Gamma_0 \geqslant 5$) $\mathrm{d}\hat{\Delta}/\mathrm{d}\zeta$ reaches a maximum at a height corresponding to $\Gamma = 5$, which lies below the contraction in the radius that occurs for sufficiently lazy plumes (see § 5.5).

To explain the behaviour of Γ and $\hat{\Delta}$ it is useful to consider the behaviour of the non-dimensional fluxes $\hat{\mathcal{G}}$ and $\hat{\mathcal{M}}$, which is illustrated by the contour plots of $\hat{\mathcal{G}}$ and $\mathrm{d}\hat{\mathcal{G}}/\mathrm{d}\zeta$ and those of $\hat{\mathcal{M}}$ and $\mathrm{d}\hat{\mathcal{M}}/\mathrm{d}\zeta$ shown in figures 5 and 6 and figures 7 and 8, respectively. It is clear from (4.7) that the variation of momentum flux at the source ($\mathrm{d}\hat{\mathcal{M}}/\mathrm{d}\zeta|_{\zeta=0} = 2\Gamma_0/5$) strengthens as the plume source departs further from a pure jet. In contrast, the vertical variation in mass flux (non-Boussinesq case) or volume flux (Boussinesq case) immediately above the source ($\mathrm{d}\hat{\mathcal{G}}/\mathrm{d}\zeta|_{\zeta=0} = 1/2$) does not respond to the value of Γ_0.

For fountains, it is evident from figure 5 that entrainment causes a significant increase in the volume flux only if the fountain is (highly) forced, i.e. as Γ_0 approaches zero from below. The rate of change with height of $\hat{\mathcal{G}}$ decreases monotonically with

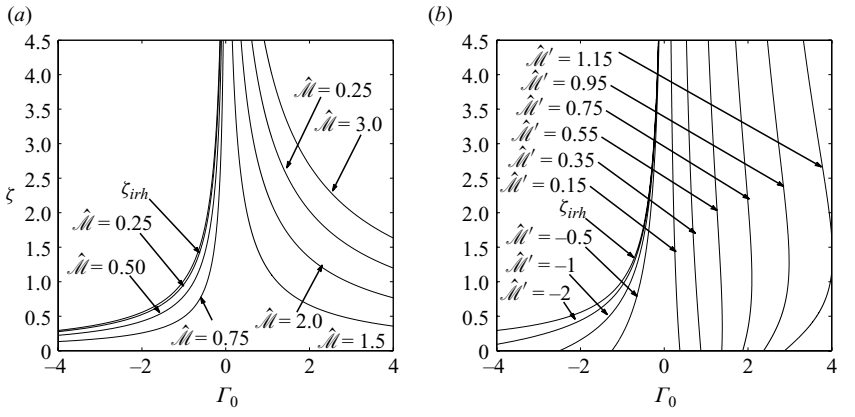

FIGURE 7. Contours of (*a*) constant $\hat{\mathscr{M}}$ and (*b*) constant $\mathrm{d}\hat{\mathscr{M}}/\mathrm{d}\zeta$, denoted by $\hat{\mathscr{M}}'$, for fountains, forced and lazy plumes.

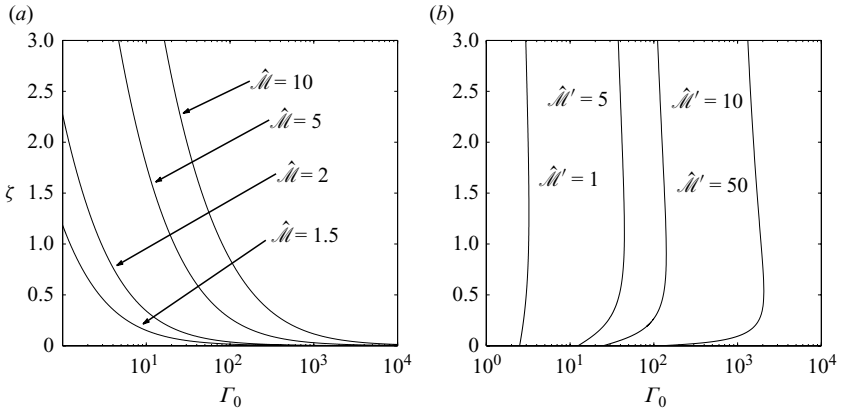

FIGURE 8. Contours of (*a*) constant $\hat{\mathscr{M}}$ and (*b*) constant $\mathrm{d}\hat{\mathscr{M}}/\mathrm{d}\zeta$, denoted by $\hat{\mathscr{M}}'$, for (very) lazy plumes.

height and converges to $\mathrm{d}\hat{\mathscr{G}}/\mathrm{d}\zeta = 0$ (cf. (4.7)) as the fountain reaches its initial rise height. For large negative values of Γ_0 (i.e. fountains with an excess of mass flux or volume flux or, alternatively, a deficit of momentum flux at the source), the momentum flux decreases very rapidly (figure 7) in contrast with the mass or volume flux, which increases only marginally (figure 5), thereby further disrupting the balance of fluxes, which converges to $\Gamma = -\infty$ over a relatively small height.

For plumes, both $\hat{\mathscr{G}}$ and $\hat{\mathscr{M}}$ increase monotonically with height. It is evident from the source values of (4.7) ($\mathrm{d}\hat{\mathscr{G}}/\mathrm{d}\zeta|_{\zeta=0} = 1/2$ and $\mathrm{d}\hat{\mathscr{M}}/\mathrm{d}\zeta|_{\zeta=0} = 2\Gamma_0/5$) and figures 5–8 that $\mathrm{d}\hat{\mathscr{G}}/\mathrm{d}\zeta$ is larger than $\mathrm{d}\hat{\mathscr{M}}/\mathrm{d}\zeta$ for forced plumes, whereas the opposite is true for lazy plumes, thus leading to a restoration of the balance of fluxes in both cases. For large (positive) values of Γ_0 (i.e. plumes with an excess of mass flux or volume flux or, alternatively, a deficit of momentum flux at the source), the momentum flux increases very rapidly in contrast with the mass or volume flux restoring the balance of fluxes, which rapidly converges towards $\Gamma = 1$ over a relatively small height. The rapid increase of momentum flux in the near-source region of very lazy plumes can also explain both the fact that $\mathrm{d}\hat{\Delta}/\mathrm{d}\zeta$ reaches a maximum in this region and the large

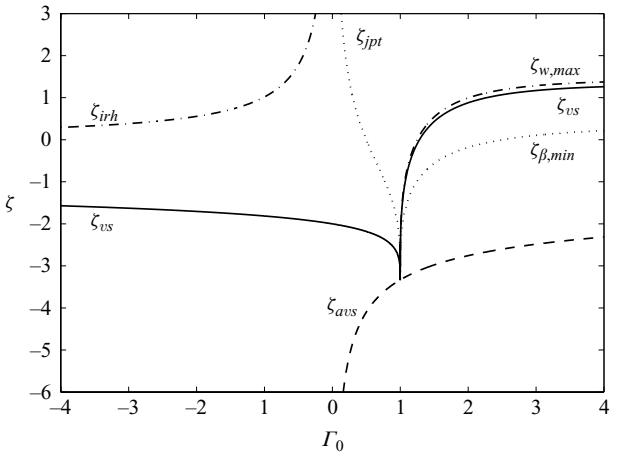

FIGURE 9. Scale diagram showing the virtual source (ζ_{vs}), the asymptotic virtual source (ζ_{avs}), the jet plume transition height (ζ_{jpt}), the minimum effective entrainment radius height ($\zeta_{\beta,min}$), the maximum vertical velocity height ($\zeta_{w,max}$) and the initial rise height (ζ_{irh}).

values $\mathrm{d}\hat{\Delta}/\mathrm{d}\zeta$ then reach. This leads to the conclusion that the density contrast with the surrounding ambient is dissipated much more rapidly in a lazy plume, which has a very rapidly increasing momentum flux despite its deficit at the source, than in a forced plume, which, in contrast, has an excess of source momentum flux. It can be shown by differentiating $\mathrm{d}\hat{\mathscr{M}}/\mathrm{d}\zeta$ in (4.7) with respect to Γ that for sufficiently lazy plumes ($\Gamma_0 \geqslant 5/4$) $\mathrm{d}\hat{\mathscr{M}}/\mathrm{d}\zeta$ reaches a minimum at a height corresponding to $\Gamma = 5/4$, which corresponds to the height at which the vertical velocity reaches a maximum (see § 5.6 and Caulfield 1991).

5. Characteristic heights

Different characteristic heights (cf. Morton & Middleton 1973) provide an insight into and give a description of the unique features of fountains and plumes. For fountains, these characteristic heights are the initial rise height (ζ_{irh}) and the virtual source (ζ_{vs}); for forced plumes, a height describing the transition from jet-like to plume-like behaviour (ζ_{jpt}), the virtual source (ζ_{vs}) and the asymptotic virtual source (ζ_{avs}); and for lazy plumes, the height at which the radius reaches a minimum ($\zeta_{b,min}$) and the height at which the velocity reaches a maximum ($\zeta_{w,max}$), in addition to the virtual source (ζ_{vs}) and the asymptotic virtual source (ζ_{avs}). We have plotted (figures 9 and 10) our generalized 'scale diagrams' to allow for direct comparison with the Boussinesq analogy in Morton & Middleton (1973), although we note that we could have plotted in addition the height corresponding to the peak in $\mathrm{d}\hat{\Delta}/\mathrm{d}\zeta$ as identified in § 4.

5.1. *Virtual source*

The virtual source exists for all values of Γ_0 and corresponds to the vertical location at which $\Gamma = 0$. For fountains ($\Gamma_0 < 0$) and forced plumes ($0 < \Gamma_0 < 1$), the virtual source can be found by evaluating the height corresponding to $\Gamma = 0$ given by (4.3). For lazy plumes ($\Gamma_0 > 1$) the upper limit of (4.3), i.e. $\Gamma = 0$, corresponding to the virtual source, lies outside the domain of validity of the integral, but the location of the virtual source can be found by integrating (4.2) across the discontinuity corresponding to

		Γ	b	w	η	$b\sqrt{\eta}$	Δ/Δ_0	Q/Q_0	G/G_0	M/M_0	$M_B/M_{B,0}$	B
B($\Gamma_0<0$)	ζ_{vs}	0	0	∞	∞	0	∞	0	$\frac{\eta_0-1}{\eta_0}$	∞	$(1-\Gamma_0)^{2/5}$	B_0
B($0<\Gamma_0<1$)	ζ_{vs}	0	0	∞	$-\infty$	0	∞	0	$\frac{\eta_0-1}{\eta_0}$	$-\infty$	$(1-\Gamma_0)^{2/5}$	B_0
NB($0<\Gamma_0<1$)	ζ_{vs}	0	0	∞	0	0	∞	$(1-\eta_0)$	0	$(1-\Gamma_0)^{2/5}$	–	B_0
B($\Gamma_0>1$)	ζ_{vs}	0	0	$-\infty$	$-\infty$	0	∞	0	$\frac{1-\eta_0}{\eta_0}$	$-\infty$	$(\Gamma_0-1)^{2/5}$	B_0
NB($\Gamma_0>1$)	ζ_{vs}	0	0	$-\infty$	0	0	∞	(η_0-1)	0	$(\Gamma_0-1)^{2/5}$	–	B_0
B($\Gamma_0>0$)	ζ_{avs}	1	0	∞	$-\infty$	0	∞	0	$\frac{\eta_0-1}{\eta_0}$	$-\infty$	0	B_0
NB($\Gamma_0>0$)	ζ_{avs}	1	0	∞	0	0	∞	$(1-\eta_0)$	0	0	–	B_0

TABLE 1. Values of the modified plume quantities and fluxes at the virtual sources (vs) for plumes and fountains and asymptotic virtual sources (avs) for plumes only in the Boussinesq (B) and the non-Boussinesq (NB) case. The subscript 0 denotes the values at the original source.

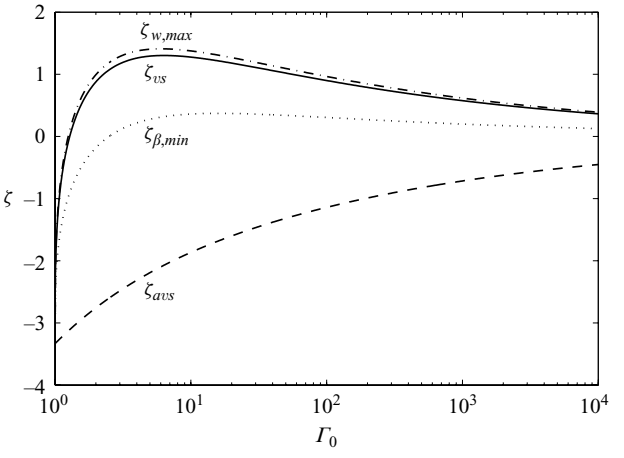

FIGURE 10. Scale diagram showing the virtual source (ζ_{vs}), the asymptotic virtual source (ζ_{avs}), the minimum effective entrainment radius height ($\zeta_{\beta,min}$) and the maximum vertical velocity height ($\zeta_{w,max}$).

$\Gamma=\pm\infty$ and taking into account the change in the sign(w) term:

$$\zeta_{vs}=\frac{(\Gamma_0-1)^{3/10}}{\sqrt{\Gamma_0}}\left(-\int_{\Gamma_0}^{\infty}\frac{\mathrm{d}\Gamma}{\sqrt{\Gamma}(\Gamma-1)^{13/10}}+\int_{-\infty}^{0}\frac{\mathrm{d}\Gamma}{\sqrt{-\Gamma}(1-\Gamma)^{13/10}}\right)\quad\text{for }\Gamma_0>1, \tag{5.1}$$

where the second integral is independent of Γ_0. The change in the sign(w) term is necessary because the virtual source of a lazy plume, as defined by Morton (1959), lies above the original source and, in physical terms, represents a fountain forced downwards against its buoyancy.

The source conditions for a modified plume or fountain, with its source located at the virtual source ($\zeta=\zeta_{vs}$) are given in table 1 for both Boussinesq and non-Boussinesq plumes and Boussinesq fountains. As the replacement plume at the virtual origin will still need to be described by the integral plume model described above, this does not simplify the problem. The virtual source is merely the first step in a two-step procedure originally developed by Morton (1959) to locate the asymptotic virtual source. As such, the virtual source evaluated herein corresponds exactly to the virtual

source evaluated by Morton (1959) for the Boussinesq case (see Appendix C) and is extended herein to include non-Boussinesq plumes. The location of the virtual source is plotted as a function of Γ_0 in figures 9 and 10.

5.2. *Asymptotic virtual source*

For forced ($0 < \Gamma_0 < 1$) and lazy plumes ($\Gamma_0 > 1$) it is clear from (4.3) that the plume will become pure ($\Gamma \to 1$) asymptotically with height. In this far-field limit, (4.3) can be simplified considerably (see Appendix D) to give:

$$\Gamma = 1 + \left(\frac{10}{3}\right)^{10/3} \left(\frac{\Gamma_0 - 1}{\Gamma_0^{5/3}}\right) (\zeta - \zeta_{avs})^{-10/3}, \tag{5.2}$$

where ζ_{avs} is the asymptotic virtual source correction. By introducing this asymptotic virtual source correction, forced and lazy plumes rising from area sources can be replaced by point source solutions that will match the original plumes asymptotically with height. By substituting the far-field expression for Γ (5.2) into (4.1), (4.4) and (4.5) the following far-field expressions are respectively obtained to the same level of approximation:

$$\begin{aligned} &\frac{\beta}{\beta_0} = \frac{3}{10}(\zeta - \zeta_{avs}), \quad \frac{w}{w_0} = \left(\frac{10}{3}\right)^{1/3} \Gamma_0^{1/3} (\zeta - \zeta_{avs})^{-1/3}, \\ &\frac{\Delta}{\Delta_0} = \left(\frac{10}{3}\right)^{5/3} \Gamma_0^{-1/3} (\zeta - \zeta_{avs})^{-5/3}. \end{aligned} \tag{5.3}$$

These expressions correspond to a pure plume from a point source of buoyancy flux only (Boussinesq case) or density deficit flux only (non-Boussinesq case) (see table 1) located at the asymptotic virtual source (Appendix D):

$$\zeta_{avs} = \begin{cases} -\dfrac{10}{3}\dfrac{1}{\sqrt{\Gamma_0}} + \dfrac{1}{\sqrt{\Gamma_0}} \displaystyle\sum_{n=1}^{n=\infty} \left(\prod_{i=1}^{i=n} (-1/2 + i) \frac{(1-\Gamma_0)^n}{(n - 3/10)n!} \right) & \text{for } 0 < \Gamma_0 \leqslant 1, \\ -\dfrac{10}{3}\dfrac{1}{\Gamma_0^{1/5}} + \dfrac{1}{\Gamma_0^{1/5}} \displaystyle\sum_{n=1}^{n=\infty} \left(\prod_{i=1}^{i=n} (-4/5 + i) \frac{\left(\frac{\Gamma_0 - 1}{\Gamma_0}\right)^n}{(n - 3/10)n!} \right) & \text{for } \Gamma_0 > 1/2, \end{cases} \tag{5.4}$$

where we note that the domain of convergence for lazy plumes ($\Gamma_0 > 1/2$) overlaps with that for forced plumes ($0 < \Gamma_0 \leqslant 1$). Figures 9 and 10 show the location of the asymptotic virtual source from (5.4) as a function of Γ_0. The far-field expressions for the plume quantities (5.3) match those from the original plume asymptotically with height and are equivalent to the solutions for pure plumes rising from area sources (3.2) for which $\zeta_{avs} = -10/3$, with the exception of the additional dependencies on Γ_0 in the expressions for w and Δ in (5.3). For pure plumes the 'asymptotic' solution is exact for all heights.

Hunt & Kaye (2001) investigated the same power-series solution for lazy Boussinesq plumes; they evaluated the minimum number n of terms of the summation required for specific values of Γ_0 for accuracy to within 1 %, 2 % and 5 %. The definition of the asymptotic virtual source (5.4) corresponds exactly to the definitions of Hunt & Kaye (2001), Morton (1959) (see Appendix C) and Carlotti & Hunt (2005) (see Appendix E), provided their lengths are scaled on the source value of the effective entrainment radius β_0.

Γ	b	w	η	$b\sqrt{\eta}$	Δ/Δ_0	Q/Q_0	G/G_0	M/M_0	$M_B/M_{B,0}$	B
$-\infty$	∞	0	$1-(1-\eta_0)\sqrt{\frac{\Gamma_0}{\Gamma_0-1}}$	∞	$\sqrt{\frac{\Gamma_0}{\Gamma_0-1}}$	$\sqrt{\frac{\Gamma_0-1}{\Gamma_0}}$	$\left(\frac{1}{\eta_0}\sqrt{\frac{\Gamma_0-1}{\Gamma_0}}-\frac{1-\eta_0}{\eta_0}\right)$	0	0	B_0

TABLE 2. Values of the quantities and fluxes for Boussinesq fountains at the initial rise height ($\zeta=\zeta_{irh}$).

5.3. *Initial rise height for fountains*

A fountain will reach a maximum height corresponding to $b\to\infty$ and $w\to 0$ and therefore to $\Gamma\to-\infty$. This rise height is termed the initial rise height (Turner 1966). The initial rise height is given by substituting $\Gamma\to-\infty$ into (4.3):

$$\zeta_{irh}=-\frac{(1-\Gamma_0)^{3/10}}{\sqrt{-\Gamma_0}}\int_{\Gamma_0}^{-\infty}\frac{\mathrm{d}\Gamma}{\sqrt{-\Gamma}(1-\Gamma)^{13/10}}. \tag{5.5}$$

It should be noted that although the use of a different entrainment coefficient for fountains can be accommodated in the vertical scaling, this solution is based on the standard plume entrainment model. Equation (5.5) is equivalent to (2.8) of Kaye & Hunt (2006) and the initial rise height definition of Morton (1959) (Appendix C). The initial rise height is plotted in figure 9. Although it is clear that the plume model becomes invalid at the initial rise height because of interaction between the upflow and the downflow at this height (cf. Bloomfield & Kerr 2000), the values of the plume quantities and fluxes in the initial rise height limit are shown in table 2, as they provide the 'source' conditions for the subsequent downflow.

5.4. *Jet plume transition*

Forced plumes undergo a transition from jet-like to plume-like behaviour. Following Morton (1959) this transition can be characterized by the average slope of the envelope for a pure jet and a pure plume. For the non-Boussinesq case the envelope of the effective entrainment radius is considered for simplicity. For a pure jet $\mathrm{d}\hat{\beta}/\mathrm{d}\zeta=1/2$, and for a pure plume $\mathrm{d}\hat{\beta}/\mathrm{d}\zeta=3/10$ (cf. (2.14)). The average of these slopes $\mathrm{d}\hat{\beta}/\mathrm{d}\zeta=2/5$ corresponds to $\Gamma=1/2$. The corresponding height as a function of Γ_0 is shown in figure 9. It should be noted that the difference in slopes of the envelopes of a pure jet and a pure plume is a feature of an entrainment model with a constant entrainment coefficient. For a ratio of the entrainment coefficients for a pure jet (α_j) and a pure plume (α_p), namely $\alpha_j/\alpha_p=3/5$, which is in close agreement with certain measured values of α_j and α_p (for example the values of Fischer *et al.* 1979, which give $\alpha_j/\alpha_p=0.64$), the slope of the envelopes of a pure jet ($\mathrm{d}\beta/\mathrm{d}z=2\alpha_j$) and a pure plume ($\mathrm{d}\beta/\mathrm{d}z=6\alpha_p/5$) are equal.

5.5. *Minimum radius*

The radius of both a Boussinesq and a non-Boussinesq plume that is sufficiently lazy will converge from its source value to a minimum at a relatively small distance above the source before expanding again with increasing height. From (2.14) this minimum radius height corresponds to $\Gamma=5/2$ for Boussinesq plumes. It should be noted that the radius neck will only occur for $\Gamma_0>5/2$. Of the characteristic heights plotted in figures 9 and 10, the height corresponding to the minimum radius is the only height that cannot be found for the non-Boussinesq case by a simple change in height scaling. In the non-Boussinesq case an expression for the radius can be obtained by

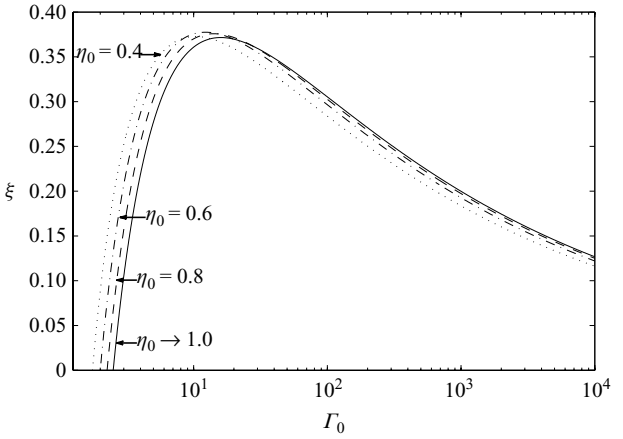

FIGURE 11. Height corresponding to the minimum radius neck for lazy non-Boussinesq plumes. The line $\eta_0 \to 1$ corresponds to the Boussinesq limit. Note that scaled height $\xi = 4\alpha z/b_0$ in this figure is different from the scaled height $\zeta = 4\alpha z/(b_0\sqrt{\eta_0})$ for the non-Boussinesq case otherwise adopted throughout the paper in order to facilitate the comparison between plumes of different η_0.

combining (4.1) and (4.5):

$$\frac{b}{b_0} = \sqrt{\eta_0}\sqrt{\frac{\Gamma}{\Gamma_0}}\left(\frac{\Gamma_0 - 1}{\Gamma - 1}\right)^{3/10}\sqrt{1 + \frac{1-\eta_0}{\eta_0}\sqrt{\frac{\Gamma_0}{\Gamma}}\sqrt{\frac{\Gamma - 1}{\Gamma_0 - 1}}}. \tag{5.6}$$

The minimum radius requires $\mathrm{d}b/\mathrm{d}\zeta = 0$, which can be evaluated in terms of a derivative of (5.6) with respect to Γ:

$$\frac{\mathrm{d}}{\mathrm{d}\zeta}\left(\frac{b}{b_0}\right) = \frac{\mathrm{d}}{\mathrm{d}\Gamma}\left(\frac{b}{b_0}\right)\frac{\mathrm{d}\Gamma}{\mathrm{d}\zeta} = 0. \tag{5.7}$$

The $\mathrm{d}\Gamma/\mathrm{d}\zeta = 0$ term in (5.7), given by (4.2), has no solutions for $\Gamma > 1$, and therefore (5.7) requires $\mathrm{d}(b/b_0)/\mathrm{d}\Gamma = 0$. From this the following implicit relationship can be obtained for Γ that is a function of η_0 and Γ_0:

$$\frac{1-\eta_0}{\eta_0}\sqrt{\frac{\Gamma_0}{\Gamma_0 - 1}} = \sqrt{\frac{\Gamma}{\Gamma - 1}}\frac{2 - \frac{4}{5}\Gamma}{1 - \left(2 - \frac{4}{5}\Gamma\right)}. \tag{5.8}$$

The solution to (5.8) can be shown to lie between the values of $\Gamma = 5/2$, corresponding to the Boussinesq limit $\eta_0 \to 1$, and $\Gamma = 5/4$, corresponding to the case in which $\Gamma_0 \to 1$ and to the case in which $\eta_0 \to 0$. Figure 11 shows the non-dimensional height $\xi = 4\alpha z/b_0$ corresponding to the minimum radius for different values of η_0 and Γ_0. It is clear from figure 11 that for smaller values of Γ_0 ($\Gamma_0 \lesssim 10$) the minimum radius will occur at greater heights in the non-Boussinesq plume compared with a plume that is Boussinesq, whereas the minimum radius will occur at smaller heights for increasingly non-Boussinesq plumes for larger values of Γ_0.

5.6. *Maximum velocity*

Above the location of the minimum radius that occurs in a sufficiently lazy plume the vertical velocity will reach its maximum value. The minimum radius and the maximum velocity do not coincide because volume is not conserved because of entrainment (Caulfield 1991). It can be shown from (2.15), in accordance with Caulfield (1991),

that the maximum velocity corresponds to $\Gamma = 5/4$. Thence, the vertical velocity will only reach a maximum value above the source for $\Gamma_0 > 5/4$. Figures 9 and 10 show the corresponding height as a function of Γ_0 for lazy non-Boussinesq and Boussinesq plumes.

6. Non-Boussinesq to Boussinesq transition

As a non-Boussinesq plume rises and entrains ambient fluid, two phenomena occur: the plume becomes pure as Γ approaches $\Gamma = 1$, and the plume, which was non-Boussinesq at the source, becomes Boussinesq as the density contrast is diluted by the entrained fluid. Woods (1997) showed that for pure plumes from point sources a characteristic length scale, on which the decrease in the density contrast between the plume and the ambient scales, naturally arises, which is a function of the density deficit flux B, the entrainment coefficient α and the gravitational acceleration g. A similar length scale can now be identified for forced and lazy plumes. Using the far-field definition of Δ (5.3) the height corresponding to a specified value of η can be expressed as

$$\xi(\Gamma_0, \eta_0, \eta) = \sqrt{\eta_0}\left(\frac{10}{3}\left(\frac{1-\eta_0}{1-\eta}\frac{\eta}{\eta_0}\right)^{3/5}\Gamma_0^{-1/5} + \zeta_{avs}\right), \tag{6.1}$$

where $\xi = 4\alpha z/b_0$ is a non-dimensional height independent of η_0. This far-field prediction of the height corresponding to a specified value of η can be compared (see figure 12) to the exact value based on numerical integration of the plume integral (4.3). By rewriting (6.1) in dimensional form, it is readily shown that the length scale measured from the asymptotic virtual source on which the convergence of η from its source value $\eta = \eta_0$ to $\eta = 1$ takes place is given by

$$L_{NB-B} \propto \frac{b_0\sqrt{\eta_0}}{4\alpha}\left(\frac{1-\eta_0}{\eta_0}\right)^{3/5}\Gamma_0^{-1/5}. \tag{6.2}$$

Substituting for Γ_0 (2.17) into (6.2), the solution identified by Woods (1997) for pure plumes rising from point sources is retrieved, namely

$$L_{NB-B} \propto \left(\frac{B_0^2}{g^3\alpha^4}\right)^{1/5}. \tag{6.3}$$

This length scale (6.3) is derived on the basis of asymptotic solutions for the far field. As a result, it can only act as a dominant length scale on which non-Boussinesq effects are important provided the far-field approximation starts to hold at a much smaller height. It can be observed from figure 12 that (6.1) gives an excellent description of the transition behaviour for lazy plumes (and improving for increasingly lazy plume sources) but not for (highly) forced plumes. The reason the length scale is not valid for highly forced plumes is that for such plumes the convergence of η from its source value $\eta = \eta_0$ to $\eta = 1$, as the plume becomes Boussinesq, is more rapid than the convergence of Γ from its source value $\Gamma = \Gamma_0$ to $\Gamma = 1$, as the plume becomes pure. The reverse is the case for lazy plumes. The contrast between the rates at which Γ converges to $\Gamma = 1$ for a forced plume and a lazy plume is also apparent from figures 1 and 2. Furthermore, it can be noted from figure 12 that the more non-Boussinesq the plume is at its source, the greater the domain of validity of the transition length scale for forced plumes.

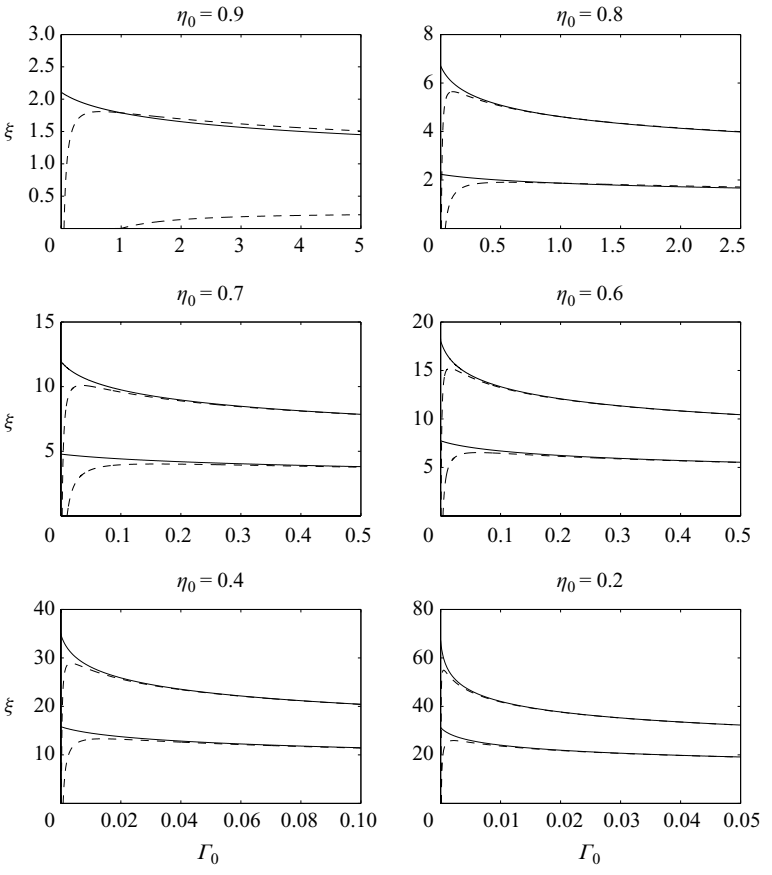

FIGURE 12. Non-Boussinesq to Boussinesq transition. Two sets of lines are plotted corresponding to $\eta = 0.95$ (upper lines) and $\eta = 0.9$ (lower lines); the continuous line corresponds to the exact height evaluated by numerical integration of (4.3), and the dashed line corresponds to the far-field approximation given by (6.1). Note that the scaled height $\xi = 4\alpha z/b_0$ is independent of η_0.

7. Conclusions

Closed-form solutions to the plume conservation equations achieved by solving for the variation with height of the non-dimensional flux balance parameter Γ, a local Richardson number, have been developed in order to describe and contrast the bulk behaviour of rising plumes and fountains from general area sources encompassing both non-Boussinesq and Boussinesq plumes and Boussinesq fountains.

The variation of contours of constant Γ, and of constant vertical rates of change of Γ, as a function of the source conditions provide further insight into the contrasting behaviours of fountains, forced plumes and lazy plumes. This insight is complemented by plotting contours of constant values of the density contrast parameter $\hat{\Delta}$, the volume (Boussinesq case) or mass (non-Boussinesq case) flux $\hat{\mathscr{G}}$ and the approximate momentum (Boussinesq case) or momentum (non-Boussinesq case) flux $\hat{\mathscr{M}}$. By scaling the height on an effective entrainment radius, 'scale diagrams' have been plotted showing characteristic heights for the different source conditions characterized by Γ_0. These scale diagrams are valid for both Boussinesq and non-Boussinesq plumes and thereby generalize the scale diagrams plotted by Morton & Middleton (1973) for

Boussinesq plumes and fountains. Morton & Middleton (1973) used a different height scaling causing the diagrams to appear markedly different; the height X plotted on their vertical axis can be related to the scaled height adopted in this paper as follows: $X = \sqrt{2/5}\sqrt{\Gamma_0}\zeta$. The only characteristic height for plumes for which the analogy between non-Boussinesq and Boussinesq releases cannot be extended by adopting an appropriate height scaling is the minimum radius neck that occurs for sufficiently lazy plumes. This case has been investigated separately, and it has been shown that the minimum radius occurs at greater heights in the non-Boussinesq plume compared with a plume that is Boussinesq for small values of Γ_0 ($\Gamma_0 \lesssim 10$), whereas it occurs at smaller heights for larger values of Γ_0. Although there is extensive experimental evidence confirming predictions of many of these characteristic heights, including the initial rise height for fountains and the asymptotic virtual source corrections for plumes, in the Boussinesq case, we note such evidence is largely absent from the literature in the non-Boussinesq case. For non-Boussinesq fountains experimental evidence is almost entirely absent, and an appropriate modified entrainment model has not been developed. Consequently, non-Boussinesq fountains are excluded from the universal solutions presented herein.

In addition it has been shown herein that the length scale on which non-Boussinesq effects are important, first identified by Woods (1997), is also valid for lazy plumes, provided it is applied from the asymptotic virtual source, but it is not valid for highly forced plumes from area sources.

This paper has shown that provided the height is scaled on the effective entrainment radius the solutions proposed herein are universally valid for Boussinesq and non-Boussinesq plumes. In doing so, this paper has shown that the results evaluated previously by various authors, who have all considered an entrainment model with a constant entrainment coefficient, for Boussinesq plumes and non-Boussinesq plumes separately are valid for both cases if the height is rescaled on the effective entrainment radius. To aid our discussion and to emphasize the universality of the solutions for both cases, the solutions proposed by different authors to the renowned model of Morton *et al.* (1956) for plumes and fountains are rewritten in the non-dimensional form adopted in this paper and provided in appendices. The generalized results obtained herein are based on an entrainment model with a constant entrainment coefficient. Plume theory with a constant α formulation has been successfully applied over many years to a range of environmental and industrial situations despite convincing evidence in the forced plume regime to support an entrainment coefficient that varies linearly with the local flux balance parameter Γ. Integrating an improved entrainment model into the framework described in this paper could potentially provide an interesting avenue for future research.

Appendix A. Pure plumes ($\Gamma_0 = 1$) from point sources

After showing that the flux of density deficiency B is conserved for slender non-Boussinesq plumes of an ideal gas, Rooney & Linden (1996) went on to use similarity considerations and dimensional arguments to show that solutions to the system of conservation equations (2.1)–(2.3) can take the following form:

$$\beta = \frac{6\alpha}{5}z, \quad w = \left(\frac{3}{4\pi}\right)^{1/3}\left(\frac{5}{6\alpha}\right)^{2/3}B^{1/3}z^{-1/3}, \quad \Delta = \frac{B^{2/3}}{g}\left(\frac{4}{3\pi^2}\right)^{1/3}\left(\frac{5}{6\alpha}\right)^{4/3}z^{-5/3}. \tag{A 1}$$

This corresponds to $\Gamma(z) = \Gamma_0 = 1$ for all heights. Using the definitions of β and Δ (see (2.16)) we note that solution (A 1) reduces exactly to the self-similar solution determined by Morton *et al.* (1956) for Boussinesq plumes.

Appendix B. Plume and fountain fluxes

The quantities β, w and Δ given by (4.1), (4.4) and (4.5), respectively, scaled on their source values and expressed in terms of Γ and Γ_0 describe all aspects of the bulk plume behaviour. These quantities can be combined to give expressions for the individual fluxes of mass, volume and momentum, which take different forms for Boussinesq and non-Boussinesq plumes. In both cases the relationship between volume flux and mass flux is straightforward, and this reflects the fluid incompressibility that is assumed in deriving the equations of motion ((2.1)–(2.3)). This relationship is given by

$$\frac{Q}{Q_0} = \eta_0 \frac{G}{G_0} + 1 - \eta_0. \tag{B 1}$$

B.1. *The non-Boussinesq case*

For non-Boussinesq plumes the fluxes of mass $G = \pi\eta w b^2$, volume $Q = \pi w b^2$ and momentum $M = \pi\eta w^2 b^2$ scaled on their respective source values can be expressed as

$$\frac{G}{G_0} = \sqrt{\frac{\Gamma}{\Gamma_0}}\sqrt{\frac{1-\Gamma_0}{1-\Gamma}}, \qquad \frac{Q}{Q_0} = \eta_0\sqrt{\frac{\Gamma}{\Gamma_0}}\sqrt{\frac{1-\Gamma_0}{1-\Gamma}} + 1 - \eta_0, \qquad \frac{M}{M_0} = \left(\frac{1-\Gamma_0}{1-\Gamma}\right)^{2/5}. \tag{B 2}$$

The rate of change of the fluxes with respect to height can be found by combining the derivatives of the fluxes (B 2) with respect to Γ with $\mathrm{d}\Gamma/\mathrm{d}\zeta$ from (4.2):

$$\left.\begin{aligned} \frac{\mathrm{d}}{\mathrm{d}\zeta}\left(\frac{G}{G_0}\right) &= \frac{1}{2}\left(\frac{1-\Gamma_0}{1-\Gamma}\right)^{1/5}, \quad \frac{\mathrm{d}}{\mathrm{d}\zeta}\left(\frac{Q}{Q_0}\right) = \frac{\eta_0}{2}\left(\frac{1-\Gamma_0}{1-\Gamma}\right)^{1/5}, \\ \frac{\mathrm{d}}{\mathrm{d}\zeta}\left(\frac{M}{M_0}\right) &= \mathrm{sign}(\Gamma)\frac{2}{5}\sqrt{\Gamma_0\Gamma}\left(\frac{1-\Gamma_0}{1-\Gamma}\right)^{1/10}. \end{aligned}\right\} \tag{B 3}$$

B.2. *The Boussinesq case*

For Boussinesq plumes the fluxes of volume $Q = \pi w b^2$ and mass $G = \pi\eta w b^2$ scaled on their respective source values are given by

$$\frac{Q}{Q_0} = \sqrt{\frac{\Gamma}{\Gamma_0}}\sqrt{\frac{1-\Gamma_0}{1-\Gamma}}, \qquad \frac{G}{G_0} = \frac{1}{\eta_0}\sqrt{\frac{\Gamma}{\Gamma_0}}\sqrt{\frac{1-\Gamma_0}{1-\Gamma}} - \frac{1-\eta_0}{\eta_0}. \tag{B 4}$$

As part of the Boussinesq approximation, the momentum flux $M = \pi\eta w^2 b^2$ is approximated by $M_B = \pi w^2 b^2$, which is given by

$$\frac{M_B}{M_{B,0}} = \left(\frac{1-\Gamma_0}{1-\Gamma}\right)^{2/5}. \tag{B 5}$$

The rate of change of the fluxes with respect to height can be found by combining the derivatives of the fluxes (B 4) and (B 5) with respect to Γ with $\mathrm{d}\Gamma/\mathrm{d}\zeta$ from (4.2):

$$\left.\begin{aligned} \frac{\mathrm{d}}{\mathrm{d}\zeta}\left(\frac{Q}{Q_0}\right) &= \frac{1}{2}\left(\frac{1-\Gamma_0}{1-\Gamma}\right)^{1/5}, \quad \frac{\mathrm{d}}{\mathrm{d}\zeta}\left(\frac{G}{G_0}\right) = \frac{1}{2\eta_0}\left(\frac{1-\Gamma_0}{1-\Gamma}\right)^{1/5}, \\ \frac{\mathrm{d}}{\mathrm{d}\zeta}\left(\frac{M_B}{M_{B,0}}\right) &= \mathrm{sign}(\Gamma)\frac{2}{5}\sqrt{\Gamma_0\Gamma}\left(\frac{1-\Gamma_0}{1-\Gamma}\right)^{1/10}. \end{aligned}\right\} \tag{B 6}$$

Although M is approximately equal to M_B under the Boussinesq approximation, a separate solution for M can be identified by including the variation in η from (4.5):

$$\frac{M}{M_0} = \frac{1}{\eta_0}\left(\frac{1-\Gamma_0}{1-\Gamma}\right)^{2/5} - \frac{1-\eta_0}{\eta_0}\sqrt{\frac{\Gamma_0}{\Gamma}}\left(\frac{1-\Gamma}{1-\Gamma_0}\right)^{1/10}. \tag{B 7}$$

Hunt & Kaye (2005) also expressed the behaviour of the volume flux Q in terms of Γ and found an expression for the near-source behaviour of lazy plumes:

$$q = \frac{Q}{Q_0} = \left(\frac{\Gamma}{\Gamma_0}\times\frac{1-\Gamma_0}{1-\Gamma}\right)^{1/2} = \left(\frac{\Gamma_0-1}{\Gamma_0}\right)^{1/2}\left(1+\frac{1}{2\Gamma}+\cdots\right) \quad \text{for } \Gamma>1. \tag{B 8}$$

To evaluate the rate of change of the non-dimensional volume flux q with height we first evaluate $\mathrm{d}q/\mathrm{d}\Gamma$ to leading order from (B 8):

$$\frac{\mathrm{d}q}{\mathrm{d}\Gamma} = -\left(\frac{\Gamma_0-1}{\Gamma_0}\right)^{1/2}\frac{1}{2\Gamma^2}. \tag{B 9}$$

Note that $\mathrm{d}\Gamma/\mathrm{d}\zeta$ is given in (4.2), and thus

$$\frac{\mathrm{d}q}{\mathrm{d}\zeta} = \frac{(\Gamma_0-1)^{1/5}}{2}\frac{(\Gamma-1)^{13/10}}{\Gamma^{3/2}}. \tag{B 10}$$

Evaluating (B 10) at the source ($\Gamma=\Gamma_0$),

$$\left.\frac{\mathrm{d}q}{\mathrm{d}\zeta}\right|_{\zeta=0} = \frac{1}{2}\left(\frac{\Gamma_0-1}{\Gamma_0}\right)^{3/2}. \tag{B 11}$$

It is clear from (B 11) that q is not constant with height, since the first derivative with height is non-zero. We note that the approximation in (B 8) is exact for $\Gamma\to\infty$. We therefore evaluate (B 11) in the limit $\Gamma_0\to\infty$ and retrieve the expected result that is consistent with (B 6):

$$\lim_{\Gamma_0\to\infty}\left(\frac{\mathrm{d}q}{\mathrm{d}\zeta}\right)\bigg|_{\zeta=0} = \frac{1}{2}. \tag{B 12}$$

Appendix C. Morton (1959)

C.1. *Virtual sources and asymptotic virtual sources*

For forced and lazy plumes, Morton (1959) evaluated the height corresponding to the virtual source (i.e. the value for which $\Gamma=0$), which is given by the following equation presented here in modified form, valid for both non-Boussinesq and Boussinesq plumes with the height scaling adopted throughout this paper:

$$\zeta_{vs} = \begin{cases} +\dfrac{5}{\sqrt{-\Gamma_0}}\displaystyle\int_{\gamma_0}^{1}\frac{v^3}{\sqrt{v^5-\gamma_0^5}}\mathrm{d}v \text{ for } \Gamma_0<0, \\ -\dfrac{5}{\sqrt{\Gamma_0}}\displaystyle\int_{\gamma_0}^{1}\frac{v^3}{\sqrt{v^5-\gamma_0^5}}\mathrm{d}v \quad \text{for } 0<\Gamma_0<1, \\ -\dfrac{5}{\sqrt{\Gamma_0}}\displaystyle\int_{-\gamma_0}^{1}\frac{v^3}{\sqrt{v^5+\gamma_0^5}}\mathrm{d}v \quad \text{for } \Gamma_0>1, \end{cases} \tag{C 1}$$

where $\gamma_0=|\Gamma_0-1|^{1/5}$ and the dummy variable $v=\sqrt{|M_B/M_{B,0}|}$. Morton (1959) used this definition of the virtual source in a two-step solution to find the more relevant

asymptotic virtual source, again represented here on a modified height scaling for consistency:

$$\zeta_{avs} = \begin{cases} -\dfrac{5}{\sqrt{\Gamma_0}}\left(\displaystyle\int_{\gamma_0}^{1} \frac{v^3}{\sqrt{v^5-\gamma_0^5}}\mathrm{d}v + 0.3343\gamma_0^{3/2}\right) & \text{for } 0<\Gamma_0<1, \\ -\dfrac{5}{\sqrt{\Gamma_0}}\left(\displaystyle\int_{-\gamma_0}^{1} \frac{v^3}{\sqrt{v^5+\gamma_0^5}}\mathrm{d}v + 1.0287\gamma_0^{3/2}\right) & \text{for } \Gamma_0>1. \end{cases} \tag{C 2}$$

C.2. *Initial rise height*

The initial rise height included in the scale diagrams of Morton & Middleton (1973) was evaluated by Morton (1959) and is given by the following equation presented here in modified form with the height scaling adopted throughout this paper:

$$\zeta_{irh} = \frac{5}{\sqrt{-\Gamma_0}}\int_0^1 \frac{v^3\mathrm{d}v}{\sqrt{|v^5-\gamma_0^5|}}, \tag{C 3}$$

where $\gamma_0 = (1-\Gamma_0)^{1/5}$.

Appendix D. Far-field expansions of plume integral

D.1. *Forced plumes*

For forced plumes the plume integral is given by (see (4.3))

$$P(\Gamma) = \int_{\Gamma_0}^{\Gamma} \frac{\mathrm{d}\Gamma}{\sqrt{\Gamma}(1-\Gamma)^{13/10}}. \tag{D 1}$$

A suitable substitution is $\phi = 1-\Gamma$, for which $\phi \to 0$ as $\Gamma \to 1$. Substituting for ϕ into (D 1) gives

$$P(\phi) = -\int_{\phi_0}^{\phi} \frac{\mathrm{d}\phi}{\phi^{13/10}\sqrt{1-\phi}}. \tag{D 2}$$

The $(1-\phi)^{-1/2}$ term of the plume integral can be expressed as a Taylor series about $\phi = 0$,

$$\frac{1}{(1-\phi)^{1/2}} = 1 + \sum_{n=1}^{n=\infty}\left(\left(\prod_{i=1}^{i=n}(-1/2+\mathrm{i})\right)\frac{\phi^n}{n!}\right), \tag{D 3}$$

which is valid for $0<\Gamma\leqslant 1$. Substituting (D 3) back into (D 1) and integrating term by term gives

$$P(\phi) = \left[\frac{10}{3}\phi^{-3/10} - \sum_{n=1}^{n=\infty}\left(\prod_{i=1}^{i=n}(-1/2+\mathrm{i})\right)\frac{\phi^{n-3/10}}{(n-3/10)n!}\right]_{\phi_0}^{\phi}. \tag{D 4}$$

Taking the leading-order term in $(1-\Gamma)$ as a far-field approximation gives Γ as a function of the non-dimensional height ζ :

$$\Gamma = 1 - \left(\frac{10}{3}\right)^{10/3}\left(\frac{1-\Gamma_0}{\Gamma_0^{5/3}}\right)(\zeta-\zeta_{avs})^{-10/3}, \tag{D 5}$$

where ζ_{avs} is the asymptotic virtual source correction,

$$\zeta_{avs} = -\frac{10}{3}\frac{1}{\sqrt{\Gamma_0}} + \frac{1}{\sqrt{\Gamma_0}}\sum_{n=1}^{n=\infty}\left(\prod_{i=1}^{i=n}(-1/2+\mathrm{i})\frac{(1-\Gamma_0)^n}{(n-3/10)n!}\right). \tag{D 6}$$

D.2. *Lazy plumes*

For lazy plumes the plume integral is given by (see (4.3))

$$P(\Gamma) = \int_{\Gamma_0}^{\Gamma} \frac{\mathrm{d}\Gamma}{\sqrt{\Gamma}(\Gamma-1)^{13/10}}. \tag{D 7}$$

A suitable substitution is $\phi = (\Gamma-1)/\Gamma$, for which $\phi \to 0$ as $\Gamma \to 1$. Substituting for ϕ in (D 7) gives

$$P(\phi) = \int_{\phi_0}^{\phi} \frac{\mathrm{d}\phi}{\phi^{13/10}(1-\phi)^{1/5}}. \tag{D 8}$$

The $(1-\phi)^{-1/5}$ term of the plume integral (D 8) can be expressed as a Taylor series about $\phi = 0$ (corresponding to $\Gamma = 1$),

$$\frac{1}{(1-\phi)^{1/5}} = 1 + \sum_{n=1}^{\infty}\left(\left(\prod_{i=1}^{i=n}(-4/5+\mathrm{i})\right)\frac{\phi^n}{n!}\right), \tag{D 9}$$

which is valid for $\Gamma > 1/2$. Substituting the power series (D 9) into the plume function (D 8) and integrating term by term gives

$$P(\phi) = \Big[-\frac{10}{3}\phi^{-3/10} + \sum_{n=1}^{\infty}\left(\left(\prod_{i=1}^{i=n}(-4/5+\mathrm{i})\right)\frac{\phi^{n-3/10}}{(n-3/10)n!}\right)\Big]_{\phi_0}^{\phi}. \tag{D 10}$$

Taking the leading-order term in $\Gamma - 1$ as a far-field approximation gives Γ as a function of the non-dimensional height ζ:

$$\Gamma = 1 + \left(\frac{10}{3}\right)^{10/3}\left(\frac{\Gamma_0 - 1}{\Gamma_0^{5/3}}\right)(\zeta - \zeta_{avs})^{-10/3}, \tag{D 11}$$

where ζ_{avs} is the asymptotic virtual source correction,

$$\zeta_{avs} = -\frac{10}{3}\frac{1}{\Gamma_0^{1/5}} + \frac{1}{\Gamma_0^{1/5}}\sum_{n=1}^{n=\infty}\left(\prod_{i=1}^{i=n}(-4/5+i)\frac{\left(\frac{\Gamma_0-1}{\Gamma_0}\right)^n}{(n-3/10)n!}\right). \tag{D 12}$$

Appendix E. Carlotti & Hunt (2005)

For forced and lazy non-Boussinesq plumes Carlotti & Hunt (2005) evaluated the height corresponding to the asymptotic virtual source. Their two-step approach is analogous to that of Morton (1959). For lazy plumes, however, Carlotti & Hunt (2005) side step the unphysical two-step correction by writing an expression for the virtual source correction in a manner analogous to that of Hunt & Kaye (2001). Their asymptotic virtual source correction, presented here in modified form with the height

scaling adopted throughout this paper, is given by

$$\zeta_{avs} = \begin{cases} -2\dfrac{(1-\Gamma_0)^{3/10}}{\sqrt{\Gamma_0}}\left(\displaystyle\int_0^{\chi}\frac{\mathrm{d}u}{(u^2+1)^{1/5}} + \omega_f\right) & \text{for } 0<\Gamma_0<1, \\ -\dfrac{10}{3}\dfrac{1}{\Gamma_0^{1/5}} + \dfrac{1}{\Gamma_0^{1/5}}\displaystyle\sum_{n=1}^{n=\infty}\left(\prod_{i=1}^{i=n}(-4/5+\mathrm{i})\frac{\left(\frac{\Gamma_0-1}{\Gamma_0}\right)^n}{(n-3/10)n!}\right) & \text{for } \Gamma_0>1/2, \end{cases} \tag{E 1}$$

where $\omega_f \approx -0.835266$ and the upper limit in the forced case $\chi = \sqrt{\Gamma_0/(1-\Gamma_0)}$. For lazy plumes this equation corresponds exactly to (5.4). For forced plumes the integral evaluated by Carlotti & Hunt (2005) can be transformed into the integral used to evaluate height in (4.3) using the substitution $u = \sqrt{\Gamma/(1-\Gamma)}$.

REFERENCES

Baines, W. D. 1983 A technique for the direct measurement of volume flux of a plume. *J. Fluid Mech.* **132**, 247–256.

Bloomfield, L. J. & Kerr, R. C. 2000 A theoretical model of a turbulent fountain. *J. Fluid Mech.* **424**, 197–216.

Carazzo, G., Kaminski, E. & Tait, S. 2006 The route to self-similarity in turbulent jets and plumes. *J. Fluid Mech.* **547**, 137–148.

Cardoso, S. S. S. & Woods, A. W. 1993 Mixing by a turbulent plume in a confined stratified region. *J. Fluid Mech.* **250**, 277–305.

Carlotti, P. & Hunt, G. R. 2005 Analytical solutions for turbulent non-Boussinesq plumes. *J. Fluid Mech.* **538**, 343–359.

Caulfield, C. P. 1991 Stratification and buoyancy in geophysical flows. PhD Thesis, University of Cambridge, Cambridge, UK.

Caulfield, C. P. & Woods, A. W. 1998 Turbulent gravitational convection from a point source in a non-uniformly stratified environment. *J. Fluid Mech.* **360**, 229–248.

Cetegen, B. M., Zukoski, E. E. & Kubota, T. 1984 Entrainment in the near field and far field of fire plumes. *Combust. Sci. Technol.* **39**, 305–331.

Conroy, D. T. & Llewellyn Smith, S. G. 2008 Endothermic and exothermic chemically reacting plumes. *J. Fluid Mech.* **612**, 291–310.

Fannelop, T. K. & Webber, D. M. 2003 On buoyant plumes rising from area sources in a calm environment. *J. Fluid Mech.* **497**, 319–334.

Fischer, H. B., List, E. J., Koh, R. C. Y., Imberger, J. & Brooks, N. H. (Eds.) 1979 *Mixing in Inland and Coastal Waters*. Academic.

Heskestad, G. 1998 Dynamics of the fire plume. *Phil. Trans. R. Soc. Lond.* A **356**, 2815–2833.

Hunt, G. R. & Kaye, N. G. 2001 Virtual origin correction for lazy turbulent plumes. *J. Fluid Mech.* **435**, 377–396.

Hunt, G. R. & Kaye, N. B. 2005 Lazy plumes. *J. Fluid Mech.* **533**, 329–338.

Kaminski, E., Tait, S. & Carazzo, G. 2005 Turbulent entrainment in jets with arbitrary buoyancy. *J. Fluid Mech.* **526**, 361–376.

Kaye, N. B. & Hunt, G. R. 2006 Weak fountains. *J. Fluid Mech.* **558**, 319–328.

Kaye, N. B. 2008 Turbulent plumes in stratified environments: a review of recent work. *Atmos.-Ocean* **46**, 433–441.

Lin, W. & Armfield, S. W. 2000 Very weak fountains in a homogeneous fluid. *Numer. Heat Transfer* A **38**, 377–396.

Linden, P. F. 1999 The fluid mechanics of natural ventilation. *Annu. Rev. Fluid Mech.* **31**, 201–238.

List, E. J. & Imberger, J. 1973 Turbulent entrainment in buoyant jets and plumes. *J. Hydraul. Div. ASCE* **99**, 1461–1474.

Morton, B. R. 1959 Forced plumes. *J. Fluid Mech.* **5**, 151–163.

Morton, B. R. 1965 Modelling fire plumes. In *Tenth Symposium (International) on Combustion*, pp. 973–982.

Morton, B. R. & Middleton, J. 1973 Scale diagrams for forced plumes. *J. Fluid Mech.* **58**, 165–176.

Morton, B. R., Taylor, G. & Turner, J. S. 1956 Turbulent gravitational convection from maintained and instantaneous sources. *Proc. R. Soc. Lond.* A **234**, 1–23.

Papanicolaou, P. N., Papakonstantis, I. G. & Christodoulou, G. C. 2008 On the entrainment coefficient in negatively buoyant jets. *J. Fluid Mech.* **614**, 447–470.

Priestley, C. H. B. & Ball, F. K. 1955 Continuous convection from an isolated source of heat. *Quart. J. R. Meteorol. Soc.* **81**, 144–157.

Ricou, F. P. & Spalding, D. B. 1961 Measurements of entrainment by axisymmetrical turbulent jets. *J. Fluid Mech.* **11**, 21–32.

Rooney, G. G. 1997 Buoyant flows from fires in enclosures. PhD Thesis, University of Cambridge, Cambridge, UK.

Rooney, G. G. & Linden, P. F. 1996 Similarity considerations for non-Boussinesq plumes in an unstratified environment. *J. Fluid Mech.* **318**, 237–250.

Scase, M. M., Caulfield, C. P. & Dalziel, S. B. 2006*a* Boussinesq plumes and jets with decreasing source strengths in stratified environments. *J. Fluid Mech.* **563**, 463–472.

Scase, M. M., Caulfield, C. P. & Dalziel, S. B. 2008 Temporal variation of non-ideal plumes with sudden reductions in buoyancy flux. *J. Fluid Mech.* **600**, 181–199.

Scase, M. M., Caulfield, C. P., Dalziel, S. B. & Hunt, J. C. R. 2006*b* Time-dependent plumes and jets with decreasing source strengths. *J. Fluid Mech.* **563**, 443–461.

Scase, M. M., Caulfield, C. P., Linden, P. F. & Dalziel, S. B. 2007 Local implications for self-similar turbulent plume models. *J. Fluid Mech.* **575**, 257–265.

Shabbir, A. & George, W. K. 1994 Experiments on a round turbulent buoyant plume. *J. Fluid Mech.* **275**, 1–32.

Thring, M. W. & Newby, M. P. 1953 Combustion length of enclosed turbulent jet flames. In *Fourth Symposium (International) on Combustion*, pp. 789–796.

Turner, J. S. 1966 Jets and plumes with negative or reversing buoyancy. *J. Fluid Mech.* **26**, 779–792.

Turner, J. S. 1979 *Buoyancy Effects in Fluids*, 2nd edn. Cambridge University Press.

Turner, J. S. 1986 Turbulent entrainment: the development of the entrainment assumption, and its application to geophysical flows. *J. Fluid Mech.* **173**, 431–471.

Wang, H. & Law, A. W-K. 2002 Second-order integral model for a round turbulent buoyant jet. *J. Fluid Mech.* **459**, 397–428.

Woods, A. W. 1997 A note on non-Boussinesq plumes in an incompressible stratified environment. *J. Fluid Mech.* **345**, 347–356.